THEORETICAL BIOLOGY AND MEDICAL MODELLING

RESEARCH Open Access

Mathematical modeling of solid cancer growth with angiogenesis

Hyun M Yang

Correspondence: hyunyang@ime.unicamp.br
UNICAMP - IMECC - DMA, Praça Sérgio Buarque de Holanda, 651, CEP: 13083-859, Campinas, SP, Brazil

Abstract

Background: Cancer arises when within a single cell multiple malfunctions of control systems occur, which are, broadly, the system that promote cell growth and the system that protect against erratic growth. Additional systems within the cell must be corrupted so that a cancer cell, to form a mass of any real size, produces substances that promote the growth of new blood vessels. Multiple mutations are required before a normal cell can become a cancer cell by corruption of multiple growth-promoting systems.

Methods: We develop a simple mathematical model to describe the solid cancer growth dynamics inducing angiogenesis in the absence of cancer controlling mechanisms.

Results: The initial conditions supplied to the dynamical system consist of a perturbation in form of pulse: The origin of cancer cells from normal cells of an organ of human body. Thresholds of interacting parameters were obtained from the steady states analysis. The existence of two equilibrium points determine the strong dependency of dynamical trajectories on the initial conditions. The thresholds can be used to control cancer.

Conclusions: Cancer can be settled in an organ if the following combination matches: better fitness of cancer cells, decrease in the efficiency of the repairing systems, increase in the capacity of sprouting from existing vascularization, and higher capacity of mounting up new vascularization. However, we show that cancer is rarely induced in organs (or tissues) displaying an efficient (numerically and functionally) reparative or regenerative mechanism.

Background

A total of 562, 875 cancer deaths were recorded in the United States in 2007, and it is estimated that approximately 570, 000 died from cancer in 2010. The overall estimate of approximately 1.53 million new cases does not include carcinoma *in situ* of any site except urinary bladder, nor does it include basal cell and squamous cell cancers of the skin. Greater than 2 million unreported cases of basal cell and squamous cell skin cancer, approximately 54, 010 cases of breast carcinoma *in situ*, and 46, 770 cases of melanoma *in situ* are expected to be newly diagnosed in 2010 [1]. In the world, the estimate for 1990 suggested a total of 8.1 million new cases, divided almost exactly between developed and developing countries, and 5.2 million cancer deaths, about 55% of which occurred in developing countries [2].

Cells of some organs, as the heart, stop proliferation after reaching their size, but others, like skin cells and cells that line body cavities, must proliferate almost continuously to replenish cells that are lost. Cancer arises when within a single cell multiple malfunctions of control systems occur, which are, broadly, the system that promote cell growth and the system that protect against erratic growth (for instance, tumor suppressor gene p53, which name comes from protein of molecular weight **53**,000, and RB, from retinoblastoma). Additional systems within the cell must be corrupted so that a cancer cell, to form a mass of any real size, produces substances (such as VEGF - Vascular Endothelial Growth Factor) that promote the growth of new blood vessels. Cellular growth-control systems can be corrupted either when cellular genes are mutated or when proteins produced during a viral infection interfere with control system function. Multiple mutations are required before a normal cell can become a cancer cell by corruption of multiple (about five) growth-promoting systems [3].

With respect to the control systems that protect against cancer, they are classified in two general types: systems that prevent mutations, and systems that deal with mutations once they occurred. For instance, there are mechanisms in cells that can convert toxic by-products of cellular metabolism or carcinogenic substances from the environment into harmless chemicals, preventing DNA damage. In addition, cells have a number of different systems that can detect damaged DNA and fix it, avoiding mutations. However, if the DNA of a cell has been damaged that repair would be impossible, there are systems which trigger the cell to die. Hence, even though there are trillions of cells, only one in three humans will get cancer during his lifetime, and cancer is mainly a disease of the elderly [3].

In order to develop effective treatments, it is important to identify the mechanisms to controlling cancer growth, how they interact, and how they can most easily be manipulated to eradicate (or manage) the disease. Aiming to gain such insight, it is usually necessary to perform large numbers of time-consuming and intricate experiments - but not always. Through the development and solution of mathematical models that describe different aspects of solid tumor growth, applied mathematics has the potential to prevent excessive experimentation and also to provide biologists with complementary and valuable insight into the mechanisms that may control the development of solid tumors [4]. In [5] it is provided a concise history of the study of tumor growth, discussing some of the most influential mathematical models and their relationship to experimental studies, and illustrating how the field of cancer research has evolved due to these interactions between theoretical and experimental approaches.

In this paper we develop a mathematical model to understand the solid cancer growth inducing angiogenesis. We determine the steady states of the model and the stability of the equilibrium points are performed. We simulate the model to assess the appearance of cancer. Treatments aiming the control of cancer are not dealt here (see [6] and [7] for tumor control).

Methods

Our objective is the development of a simple mathematical model to describe the cancer growth dynamics inducing angiogenesis. The model does not include important physiological processes like the diffusion of oxygen into a solid where it is consumed by metabolic processes, the outward diffusion of lactic acid from a solid which

produces it by metabolic processes and the diffusion of oxygen away from a blood vessel into a region with an oxygen debt. First, we describe an organ of human body free of cancer and, then, cancer cells appear in this organ.

The normal cells of an organ (the concentration at time t is designed as C) are feed by an existing vasculature formed by endothelial cells (the concentration at time t is designed as E). Adult endothelial cells and cells of an organ of human body are normally quiescent apart from certain developmental processes (e.g., embryogenesis), and proliferation of these cells aims to replenish losses (for instance, cells dying due to aging and wound). The normal cells and surrounding vascular networks (epithelial cells) are governed by the logistic growth, with intrinsic growth rates α_1 and α_2, respectively, and they are under mortality rates μ_1 and μ_2, respectively. Normal cells produce substances to promote the growth of blood vessels in a suitable network to attend their needs. The extension of vascularization (blood vessels network) depends on the size and function of the organ, and conversely, the blood vessels network determines the activity of the organ. In other words, the size of an organ could be determined by the surrounding network of blood vessels, that is, $k_1(E)$, as k_2 depends on C, $k_2(C)$, where k_1 and k_2 are the carrying capacities of the organ (normal cells) and the extension of blood vessels network (epithelial cells), respectively. In a cancer free state, normal cells (C) and blood vessels (E) are in a steady state, where the amount of normal cells depends on the feeding network, as well as the amount of epithelial cells depends on the size and function of organs that must feed.

Let us suppose that a series of accumulating mutations in normal cells (one single cell may be sufficient) corrupted systems that promote cell growth and that protect against erratic growth. Also systems that control the production of substances which induce new blood vessels are corrupted in the cancer cells. These sequential events initiate a rapid growth of cancer due to angiogenesis. Angiogenesis is the process by which new blood vessels develop from an existing vasculature, through endothelial cell sprouting, proliferation, and fusion [8]. The angiogenesis links the relatively harmless avascular and the potentially fatal vascular growth phases of the tumor [9].

Let us consider what occurs in cancer growth: (1) there is an initial amount of cancer cells (the model does not deal with the origin of cancer cells) appearing in a completely health organ; (2) these cells induce the formation of pre-vascular cells from existing vascular network; (3) after a period of time, the formation of new blood vessels is initiated; and (4) both normal and cancer cells compete for nutrients and space (proteins, oxygen, etc.).

For cancer cells (the concentration at time t is designed as T), the growth, which is likely to be limited by energetic constraints, is limited by the carrying capacity k_3 and the surrounding new vessels originated by angiogenesis (the concentration at time t is designed as A). The new vessels, represented by angiogenesis cells A, have growth depending on tumor cells T and are limited by available space (k_4). The growth of blood vessels (E and A) are constrained by physical restrictions, even they are never subject to either oxygen or nutrient deprivation. We assume the existence of an early stage of angiogenesis, called pre-angiogenesis (the concentration of cells at time t is designed as P). This stage corresponds to the release by tumoral cells of VEGF, which starts to diffuse into the surrounding tissue and approach the endothelial cells of nearby blood vessels. Endothelial cells subsequently respond to the VEGF concentration gradient by forming sprouts. From these sprouts, there occur migration and

proliferation toward the tumor, and these new vessels are called as angiogenesis (endothelial cells A).

The tumoral cells induce new vascular network from the existing one to feed cancer cells. The pre-angiogenesis cells are formed by the mass action law [10] at a constant rate γ, the rate of sprouts formation, from which new vascularizations occur resulting in angiogenesis cells after an average period of time δ^{-1}, where δ is transfer rate from pre-angiogenesis to angiogenesis cells. The cancer, pre-angiogenesis and angiogenesis cells are under the mortality rates μ_3, μ_4 and μ_5, respectively. The cancer and angiogenesis cells are governed by the logistic growth: intrinsic growth α_3 and ε, which depend respectively on angiogenesis and cancer cells, and carrying capacities k_3 and k_4, respectively. Cancer cells can also grow logistically using existing vascularization at rate α'_3. The rates at which normal and cancer cells compete themselves for resources and space are β'_1 and β'_2. Both parameters also take into account effects of the environment.

Pre-angiogenesis cells deserve some words. New blood vessels to nourish cancer cells must sprout from pre-existing blood vessels. However, there is an elapse of time from the appearance of sprouts until the complete formation of new blood vessels that effectively feed cancer cells. By doing this, we take into account a time-delay between the formation of new network of blood vessels (angiogenesis cells A) and tumor growth. Notice that the probability of sproutings becoming angiogenesis cells is $\delta/(\delta + \mu_4)$. If we let $\delta \to \infty$, this phase is negligible (probability one).

Let us consider the normal cells C taking into account the above descriptions. In the absence of cancer cells T, normal cells obey $\frac{d}{dt}C = \alpha_1 C[1 - \frac{C}{k_1(E)}] - \mu_1 C$. The cancer cells influence negatively normal cells, and this term is described by $\frac{\alpha_1 C\beta'_1 T}{k_1(E)}$ with negative signal. Due to mutation, some normal cells become cancer cells, which can occur continuously. However, we will assume that the mutations occur instantaneously at a given time (cancer cells grow exponentially in the beginning, hence further mutations, being in small amount, can be disregarded), when an amount of normal cells are transferred to cancer cells compartment. For other types of cells, the dynamical equations can be obtained similarly.

Based on the above definitions of variables and model's parameters, the dynamics of the cancer growth is described by the following system of equations

$$\begin{cases} \frac{d}{dt}C = \alpha_1 C\left[1 - \frac{C}{k_1(E)} - \frac{\beta'_1 T}{k_1(E)}\right] \\ \qquad -\mu_1 C - C_m\delta_D(t) \\ \frac{d}{dt}E = \alpha_2 E\left[1 - \frac{E}{k_2(C)}\right] - \gamma ET - \mu_2 E \\ \frac{d}{dt}T = C_m\delta_D(t) + \alpha_3 AT\left(1 - \frac{T}{k_3}\right) \\ \qquad +\alpha'_3 T\left[1 - \frac{T}{k_1(E)} - \frac{\beta'_2 C}{k_1(E)}\right] - \mu_3 T \\ \frac{d}{dt}P = \gamma ET - \delta P - \mu_4 P \\ \frac{d}{dt}A = \delta P + \varepsilon TA\left(1 - \frac{A}{k_4}\right) - \mu_5 A. \end{cases}$$

In this model, an amount C_m of normal cells are mutated to cancer cells at time $t = 0$, which is described by the Dirac delta function $\delta_D(t)$: it assumes ∞ at $t = 0$, and 0, otherwise.

Let us simplify the model assuming that k_1 and k_2 are constant, depending only on the status corresponding to cancer free. Under this simplification, we can define the interaction parameters as $\beta_1 = \beta_1'\alpha_1/k_1$ and $\beta_2 = \beta_2'\alpha_3'/k_1$. Another simplification assumes that the rate at which cancer cells increase due to new vascularization is much higher than due to existing one, or we let $\alpha_3 AT(1 - T/k_3) \gg \alpha_3' T(1 - T/k_1)$. The above impulsive system taking into account these simplifications can be written as, for $t > 0$,

$$\begin{cases} \frac{d}{dt}C = \alpha_1 C\left(1 - \frac{C}{k_1}\right) - \beta_1 CT - \mu_1 C \\ \frac{d}{dt}E = \alpha_2 E\left(1 - \frac{E}{k_2}\right) - \gamma ET - \mu_2 E \\ \frac{d}{dt}T = \alpha_3 AT\left(1 - \frac{T}{k_3}\right) - \beta_2 CT - \mu_3 T \\ \frac{d}{dt}P = \gamma ET - \delta P - \mu_4 P \\ \frac{d}{dt}A = \delta P + \varepsilon TA\left(1 - \frac{A}{k_4}\right) - \mu_5 A, \end{cases} \tag{1}$$

in order to describe a perturbation introduced at $t = 0$ in a cancer free status. Hence, the initial conditions supplied to the system of equations become:

$$\begin{aligned} &(C(0) = C_0 - C_m, E(0) = E_0, \\ &T(0) = C_m, P(0) = 0, A(0) = 0), \end{aligned} \tag{2}$$

where C_0 and E_0 are the cancer free steady state values (see below), and C_m is the instantaneous mutation of normal cells to initiate cancer growth. The vital dynamics of normal cells is similar than that presented in [11]. In Table 1 we present the summary of variables, which depend on time, for instance $C(t)$, and parameters, which do not depend on time, of the model.

We next obtain the steady states of the system of equations (1), and the corresponding characteristic equations in order to establish the stability of the steady states.

Steady states

We determine the steady states of the system (1), denoted by $\bar{Q} = (\bar{C}, \bar{E}, \bar{T}, \bar{P}, \bar{A})$. The coordinates of the equilibrium point are obtained by letting the time derivatives in equation (1) equal to zero, for instance, $\frac{d}{dt}C = 0$. The first is the equilibrium where there is not any cells, that is,

$$\bar{Q}^{abs} = (0, 0, 0, 0, 0).$$

For obvious reason, this point is not considered here.

The trivial equilibrium point, given by

$$\bar{Q}^0 = (C_0, E_0, 0, 0, 0),$$

Table 1 Symbols and definitions

Symbols	Definitions
C	Concentration of normal cells at time t
E	Concentration of epithelial cells at time t
T	Concentration of cancer cells at time t
P	Concentration of pre-angiogenesis cells at time t
A	Concentration of angiogenesis cells at time t
α_1	Intrinsic growth rate of normal cells
α_2	Intrinsic growth rate of epithelial cells
α_3	Intrinsic growth rate of cancer cells
ε	Intrinsic growth rate of angiogenesis cells
μ_1	Mortality rate of normal cells
μ_2	Mortality rate of epithelial cells
μ_3	Mortality rate of cancer cells
μ_4	Mortality rate of pre-angiogenesis cells
μ_5	Mortality rate of angiogenesis cells
k_1	Carrying capacity of normal cells
k_2	Carrying capacity of epithelial cells
k_3	Carrying capacity of cancer cells
k_4	Carrying capacity of angiogenesis cells
δ	Transfer rate from pre-angiogenesis to angiogenesis cells
γ	Epithelial sprouting rate
β_1	Rate of inhibition of normal cells by cancer cells
β_2	Rate of inhibition of cancer cells by normal cells

The summary of the variables and parameters of the model.

where C_0 and E_0 are

$$\begin{cases} C_0 = \dfrac{k_1}{\alpha_1}(\alpha_1 - \mu_1) \\ E_0 = \dfrac{k_2}{\alpha_2}(\alpha_2 - \mu_2), \end{cases} \tag{3}$$

corresponds to the absence of cancer. The trivial equilibrium point exists for $\alpha_1 > \mu_1$ and $\alpha_2 > \mu_2$. In this model the normal and epithelial cells are not dependent on each other. One possibility of dependence can be done by the carrying capacities $k_1(E_0)$ and $k_2(C_0)$.

The coordinates of the non-trivial equilibrium point $\bar{Q}^*$ are

$$\begin{cases} \bar{C} = \dfrac{k_1}{\alpha_1}[(\alpha_1 - \mu_1) - \beta_1 \bar{T}] \\ \bar{E} = \dfrac{k_2}{\alpha_2}[(\alpha_2 - \mu_2) - \gamma \bar{T}] \\ \bar{P} = \dfrac{\gamma k_2}{(\mu_4 + \delta)\alpha_2}[(\alpha_2 - \mu_2) - \gamma \bar{T}]\bar{T} \\ \bar{A} = \dfrac{k_3}{k_3 - \bar{T}}\left[\dfrac{\mu_3}{\alpha_3} + \dfrac{\beta_2 k_1}{\alpha_3 \alpha_1}(\alpha_1 - \mu_1) - \dfrac{\beta_1 \beta_2 k_1}{\alpha_3 \alpha_1}\bar{T}\right], \end{cases} \tag{4}$$

where $\bar{T}$ is the positive solution of the equation

$$f(T) = g(T) \equiv g_1(T) + g_2(T), \tag{5}$$

with the fourth degree polynomial $f(T)$, and the third degree polynomials $g_1(T)$ and $g_2(T)$ being given by

$$\begin{cases} f(T) = \dfrac{\gamma\delta k_2}{(\mu_4+\delta)\mu_5\alpha_2 k_3}[(\alpha_2-\mu_2)-\gamma T] \\ \qquad \times(k_3-T)^2 T \\ g_1(T) = \left(1-\dfrac{\varepsilon}{\mu_5}T\right)(k_3-T) \\ \qquad \times\left[\dfrac{\mu_3}{\alpha_3}+\dfrac{\beta_2 k_1}{\alpha_3\alpha_1}(\alpha_1-\mu_1)-\dfrac{\beta_1\beta_2 k_1}{\alpha_3\alpha_1}T\right] \\ g_2(T) = \dfrac{\varepsilon k_3}{\mu_5 k_4}T \\ \qquad \times\left[\dfrac{\mu_3}{\alpha_3}+\dfrac{\beta_2 k_1}{\alpha_3\alpha_1}(\alpha_1-\mu_1)-\dfrac{\beta_1\beta_2 k_1}{\alpha_3\alpha_1}T\right]^2. \end{cases} \tag{6}$$

By inspecting $\bar{C}$, $\bar{E}$ and $\bar{A}$, the positive solution $\bar{T}$, in order to $\bar{Q}^*$ be biologically feasible, must satisfy, respectively, the constraints $\bar{T} < T_C, \bar{T} < T_E$ and $\bar{T} < T_A$, where

$$\begin{cases} T_C = \dfrac{\alpha_1-\mu_1}{\beta_1} \\ T_E = \dfrac{\alpha_2-\mu_2}{\gamma} \\ T_A = k_3. \end{cases} \tag{7}$$

However, the constraint for the equilibrium $\bar{A}$ is $\bar{T} < T_g$, where

$$\begin{aligned} T_g &= \frac{\alpha_1\alpha_3}{\beta_1\beta_2 k_1}\left[\frac{\mu_3}{\alpha_3}+\frac{\beta_2 k_1}{\alpha_3\alpha_1}(\alpha_1-\mu_1)\right] \\ &= \frac{\alpha_1\mu_3}{\beta_1\beta_2 k_1}+\frac{\alpha_1-\mu_1}{\beta_1}, \end{aligned} \tag{8}$$

but it is always satisfied when $\bar{T} < T_C$, since $T_g > T_C$.

With respect to the constraints, we must have $\bar{T} < \min\{T_C, T_E, T_A\}$, where $\min\{T_C, T_E, T_A\}$ is the minimum among T_C, T_E and T_A. The constraints depend inversely with removing parameters β_1 and γ, and directly with the carrying capacity k_3. Hence, for higher values of removing parameters β_1 and γ, and lower values of carrying capacity k_3, the constraints are decreased, that is, the steady state cancer cells $\bar{T}$ must assume lower values. Let us suppose that k_3 is high, which implies that cancer cells $\bar{T}$ can achieve higher values. If the sproutings rate γ from existing blood vessels is high, in principle it seems to be beneficial to cancer cells. However, higher values of γ result in lower values for the constraint T_E, and, consequently, $\bar{T}$ must assume lower values, because it must be lower than both T_E and k_3. Therefore, cancer cells will achieve higher values for high carrying capacity k_3, and lower sprouting rate γ. Further angiogenesis cells must be originated by the clonal division from a small amount of pre-angiogenesis cells. In appendix A we show the analysis of equation (5). Summarizing, the number of solutions $\bar{T}$ depends on the values assigned to the model's parameters, which can be 0, 2 or 4. Notwithstanding, the solution $\bar{T}$ must obey the constraints given in equation (7), which reduces the number of solutions up to 2. In the case of 2

solutions, we denote the solutions $\bar{T}$ as small ($T_<$, and the corresponding equilibrium point $\bar{Q}^*_<$) and big ($T_>$, and the corresponding equilibrium point $\bar{Q}^*_>$). Hence, the constraints play an important role in the number of equilibrium points. Notice that the interacting parameter ε does not appear in the constraints. Let us analyze possible scenarios resulting by varying the non-linear term parameters β_1, β_2, γ and ε. First, let us vary β_1. Notice that T_C depends on β_1, but T_E and T_A do not. For small β_1, the solution $\bar{T}$ of equation (5) situates below T_C. However, as β_1 increases, $\bar{T}$ can surpass T_C, after intercepting T_C at $\beta_1 = \beta_1^c$. As $\bar{T}$ increases with β_1, $\bar{C}$, given by the first equation of (4), decreases and reaches zero at $\beta_1 = \beta_1^c$, and $\bar{C} < 0$ sinceafter. At $\beta_1 = \beta_1^c$ we have $\bar{T} = T_C^c = (\alpha_1 - \mu_1)/\beta_1^c$. Let us suppose that $T_C^c < \min\{T_E, T_A\}$, the minimum between T_E and T_A. When $\bar{C} = 0$, there arises another feasible equilibrium point $\bar{Q}^c$, with the coordinates

$$\begin{cases} \bar{C} = 0 \\ \bar{E} = \dfrac{k_2}{\alpha_2}\left[(\alpha_2 - \mu_2) - \gamma\bar{T}\right] \\ \bar{P} = \dfrac{\gamma k_2}{(\mu_4 + \delta)\alpha_2}\left[(\alpha_2 - \mu_2) - \gamma\bar{T}\right]\bar{T} \\ \bar{A} = \dfrac{k_3\mu_3}{\alpha_3(k_3 - \bar{T})}, \end{cases} \tag{9}$$

where $\bar{T} = T_C^c$, and the equilibrium $\bar{T}$ does not depend anymore on the interacting parameter β_1. Hence for $\beta_1 \geq \beta_1^c$ we have a constant value $\bar{T} = (\alpha_1 - \mu_1)/\beta_1^c$, which implies in constant values for $\bar{E}$, $\bar{P}$ and $\bar{A}$.

See more discussion below, in the stability analysis.

The equilibrium point $\bar{Q}^c$ corresponds to the case where the cancer cells displaced normal cells. By inspecting the equation for $\bar{C}$, the first in equation (4), the normal cells drop out to zero for a sufficiently higher values of β_1. In another words, when cancer cells have very higher fitness than normal cells and overcome the competition for resources, they can lead to the exclusion of the normal cells (of course, the cancer diseased person dies before reaching this equilibrium). Notice that $\bar{Q}^c$ can be avoided as the equilibrium point when k_3 assumes small values, that is, if $k_3 < \min\{T_E, T_C\}$, minimum between T_E and T_C. In this situation, the equilibrium value $\bar{T}$ is always smaller than k_3, and all coordinates of the equilibrium point are positive (Appendix A).

Second, let us now vary β_2. The third equation of (1) in the equilibrium can be written as

$$\bar{T} = \frac{k_3}{\bar{A}\alpha_3}\left[(\bar{A}\alpha_3 - \mu_3) - \beta_2\bar{C}\right].$$

When β_2 increases, $\bar{T}$ decreases, and at a certain value of β_2, say β_2^{th}, $\bar{T}$ assumes zero value. When $\bar{T} = 0$, the unique feasible equilibrium point is the trivial $\bar{Q}_0$. When the influence of the normal cells and the environment is higher ($\beta_2 \geq \beta_2^{th}$), then cancer can not be maintained.

Cancer onset depends on the interplay among the initial condition $T(0) = C_m$ and interacting parameters β_1 and β_2. Once cancer cells are originated by mutation from several sources, these cells interact with healthy cells and the surrounding environment. While the parameter β_1 is practically insensitive in the behavior of the dynamics, however, there is a threshold in the parameter β_2, above which cancer can not be established. This result shows that cancer is rarely induced in organs (or tissues) displaying an efficient (numerically and functionally) reparative or regenerative mechanism [12], which is the reason for the incidence of cancer rising exponentially with age [13].

Finally, let us analyze the effects of varying the sprouting rate γ and angiogenesis increasing rate ε.

When γ increases, $\bar{E}$ decreases according to the second equation of (4). Let us assume that $\bar{E}$ reaches zero at a certain value named γ^f, and $\bar{E} < 0$ sinceafter. When $\bar{E} = 0$, differently from $\bar{C} = 0$, the unique feasible equilibrium point is the trivial $\bar{Q}_0$. Hence, we expect that $\bar{E} > 0$ for $\gamma \geq 0$, because of $\bar{T} < T_E = (\alpha_2 - \mu_2)/\gamma$ is always obeyed, and there is not a critical value γ^f. When we decrease γ, we observe that equation (5) may not have biologically feasible solutions.

Initially, let us analyze $\gamma = 0$. In this case, we have $f(T) = 0$, and the equilibrium value $\bar{T}$ is solution of the polynomial of degree two

$$0 = \left(1 - \frac{\varepsilon}{\mu_5}T\right)(k_3 - T) + \frac{\varepsilon k_3}{\mu_5 k_4}T \times \left[\frac{\mu_3}{\alpha_3} + \frac{\beta_2 k_1}{\alpha_3 \alpha_1}(\alpha_1 - \mu_1) - \frac{\beta_1 \beta_2 k_1}{\alpha_3 \alpha_1}T\right], \tag{10}$$

with another being given by $\bar{T} = T_g$. Moreover, from equation (4), we have $\bar{P} = 0$ (due to $\gamma = 0$, the role of the parameter δ does not matter). In this case, there arises another feasible equilibrium point $\bar{Q}^p$, with the coordinates

$$\begin{cases} \bar{C} = \dfrac{k_1}{\alpha_1}[(\alpha_1 - \mu_1) - \beta_1 \bar{T}] \\ \bar{E} = \dfrac{k_2}{\alpha_2}(\alpha_2 - \mu_2) \\ \bar{P} = 0 \\ \bar{A} = \dfrac{k_3}{k_3 - \bar{T}}\left[\dfrac{\mu_3}{\alpha_3} + \dfrac{\beta_2 k_1}{\alpha_3 \alpha_1}(\alpha_1 - \mu_1) - \dfrac{\beta_1 \beta_2 k_1}{\alpha_3 \alpha_1}\bar{T}\right]. \end{cases} \tag{11}$$

Equation (10) has two positive solutions (not shown) when $T_g > k_3$ and $\varepsilon > \mu_5/k_3$, where T_g is given by equation (8), while a unique positive solution occurs when $T_g = k_3$. Let us introduce a threshold of ε, named ε^{th}. We remark that this threshold value appears only for $\gamma = 0$. Hence, when $\varepsilon > \varepsilon^{th}$, with $\varepsilon^{th} > \mu_5/k_3$, we have two positive solutions, named $T^{\varepsilon}_{<}$ (and the corresponding equilibrium point $\bar{Q}^p_{<}$) and $T^{\varepsilon}_{>}$ (and the corresponding equilibrium point $\bar{Q}^p_{>}$), which collapse to one at $\varepsilon = \varepsilon^{th}$, and for $\varepsilon < \varepsilon^{th}$ there is not positive solution. The equilibrium point $\bar{Q}^p$ represents the origin of angiogenesis from other sources, not from existing vascular system feeding an organ of the human body. Two facts must occur to appearing of $\bar{Q}^p$: sufficiently higher capacity of

cancer cells to originate new vascular system from external sources ($\varepsilon > \varepsilon^{th}$), and higher initial amount, at time 0, of vascular cells $(T(0) > T^{\varepsilon}_{<})$.

Now, for lower values of γ ($\gamma \geq 0$), as a consequence of the appearing of ε^{th} for $\gamma = 0$, equation (5) does not have positive solution and there is not biologically feasible equilibrium point. Let us introduce a threshold of γ, named γ^{th}. For $\gamma < \gamma^{th}$ the unique solution is $\bar{T} = 0$ (this fact is shown numerically). Note that as ε increases, γ^{th} decreases. Hence, higher the capacity of building up new vascularization ε, less the amount of sprouts originated from existing blood vessels needed to angiogenesis. In the special case $\varepsilon = 0$ (cancer cells do not promote growth in the new vascularization), the equilibrium $\bar{T}$, which must be substituted in the variables given in equation (4), must be solution of $f(T) = g(T)$, where

$$\begin{cases} f(T) = \dfrac{\gamma \delta k_2}{(\mu_4 + \delta)\mu_5 \alpha_2 k_3}[(\alpha_2 - \mu_2) - \gamma T] \\ \qquad \times (k_3 - T)T \\ g(T) = \dfrac{\mu_3}{\alpha_3} + \dfrac{\beta_2 k_1}{\alpha_3 \alpha_1}(\alpha_1 - \mu_1) - \dfrac{\beta_1 \beta_2 k_1}{\alpha_3 \alpha_1} T. \end{cases} \tag{12}$$

This equation clearly shows that a positive solution $\bar{T}$ is feasible for sufficiently higher values of γ, that is, $\gamma > \gamma_0^{th}$, where γ_0^{th} corresponds to $\varepsilon = 0$. Due to the fact that ε increases as γ^{th} decreases, γ_0^{th} is the upper bound of the threshold of γ. Even the cancer cells do not promote the proliferation of the sprouted endothelial (pre-angiogenesis) cells ($\varepsilon = 0$), if the capacity of endothelial cell sprouting is higher ($\gamma > \gamma^{th}$), then cancer cells can be maintained.

There are two mechanisms by which the tumor's vasculature is built: (1) as a tumor grows, it excretes tumor angiogenesis factor, which help activate endothelial cells of nearby blood vessels, initiating angiogenesis; (2) bone marrow derived endothelial progenitor cells are mobilized into the blood, by means of long-range signaling, and they are recruited from blood by the tumor by short-range signaling, resulting in vasculogenesis (the vascular endothelium of the nearby vessels become activated and allows the endothelial progenitor cells to extravase and start a cycle of differentiation/division) [14]. In both cases, the newly stimulated endothelial cells (described by parameter γ) and the recruited endothelial progenitor cells (this phenomenon is not considered in the model; however, the case $\gamma = 0$ can in some extent be understood as vasculogenesis) enter a stage of clonal expansion and continue to form blood vessels, which is described by the parameter ε.

With respect to the linear term of the pre-angiogenesis parameter δ, when $\delta \to \infty$, $\bar{Q}^{\infty}$ appears, similar to the equilibrium point $\bar{Q}^{p}$, because $\lim_{\delta \to \infty} \bar{P} = 0$. However, from the third equation of (4), we have $\lim_{\delta \to \infty} \delta \bar{P} = \gamma \bar{E} \bar{T}$. Hence, the coordinates of $\bar{Q}^{\infty}$ are those given in equation (11), but $\bar{T}$ is solution of the equation $f(T) = g_1(T) + g_2(T)$, where

$$f(T) = \frac{\gamma k_2}{\mu_5 \alpha_2 k_3}[(\alpha_2 - \mu_2) - \gamma T](k_3 - T)^2 T,$$

and $g_1(T) + g_2(T)$ is given be equation (6). Notice that $f(T)$ differs from that in equation (6) by the factor $\delta/(\mu_4 + \delta)$. The equilibrium point $\bar{Q}^{\infty}$ represents the absence of the intermediate pre-angiogenesis, that is, angiogenesis occurs directly and instantaneously from epithelial cells.

Summarizing, the non-trivial equilibrium points $\bar{Q}^*$ ($\bar{Q}^*_<$ and $\bar{Q}^*_>$, when they exist), $\bar{Q}^c$ (for $\beta_1 \geq \beta_1^c$), and $\bar{Q}^p$ (when $\gamma = 0$) are biologically feasible, but $\bar{Q}^c$ is not a real cancer equilibrium point, since $\bar{C} = 0$. Especially, $\bar{Q}^p$ is a cancer equilibrium point only if vasculogenesis can act alone to generate new blood vessels. The analysis of the model showed the existence of thresholds β_2^{th} and γ^{th} (and, eventually, ε^{th}, for $\gamma = 0$), and a critical value β_1^c.

We analyzed the steady states of the model described by the system of ordinary differential equations (1) assuming that all parameters of the linear terms (μ_1, μ_2, μ_3, μ_4, μ_5 and δ) plus the intrinsic growth rates α_1, α_2 and α_3 and carrying capacities k_1, k_2, k_3 and k_4 are fixed values. But, the parameters regarded to the interaction between different cells (β_1, β_2, γ and ε) are generally unknown, hence they were allowed to vary to analyze broad range of variation in these parameters.

Local stability analysis

The local stability of the equilibrium points [15] is determined by the eigenvalues of the characteristic equation $\det(\bar{J} - \lambda I) = 0$, where $\bar{J}$ is the Jacobian J evaluated at the equilibrium point under analysis,

$$\bar{J} = \begin{bmatrix} -\frac{\alpha_1}{k_1}\bar{C} & 0 & -\beta_1\bar{C} & 0 & 0 \\ 0 & -\frac{\alpha_2}{k_2}\bar{E} & -\gamma\bar{E} & 0 & 0 \\ -\beta_2\bar{T} & 0 & -\frac{\alpha_3}{k_3}\bar{A}\bar{T} & 0 & j_1 \\ 0 & \gamma\bar{T} & \gamma\bar{E} & -j_2 & 0 \\ 0 & 0 & j_3 & \delta & -j_4 \end{bmatrix}$$

where j_1, j_2, j_3 and j_4 are

$$\begin{cases} j_1 = \alpha_3\bar{T}\left(1 - \dfrac{\bar{T}}{k_3}\right) \\ j_2 = \mu_4 + \delta \\ j_3 = \varepsilon\bar{A}\left(1 - \dfrac{\bar{A}}{k_4}\right) \\ j_4 = \delta\dfrac{\bar{P}}{\bar{A}} + \dfrac{\varepsilon}{k_4}\bar{A}\bar{T}. \end{cases} \tag{13}$$

The Jacobian $\bar{J}$ was obtained using equilibrium equations given in (4) assuming that $\bar{C} \neq 0$. When $\bar{C} = 0$, the element in the first line and first column is $a_{11} = (\alpha_1 - \mu_1) - \beta_1\bar{T}$, and in the third column, $a_{13} = 0$.

We present analytical results corresponding to the equilibrium points $\bar{Q}^0$ and $\bar{Q}^c$.

The eigenvalues (from Jacobian $\bar{J}^0$) corresponding to the trivial equilibrium point $\bar{Q}^0$ are: $\lambda_1 = -\mu_5$, $\lambda_2 = -(\mu_4 + \delta)$, $\lambda_3 = -(\mu_3 + \beta_2 C_0)$, $\lambda_4 = -(\alpha_1 - \mu_1)$, and $\lambda_5 = -(\alpha_2 - \mu_2)$.

In the last two eigenvalues we used the coordinates given by equation (3). Hence, the trivial equilibrium $\bar{Q}^0$ is locally asymptotically stable whenever this point exists ($\alpha_1 > \mu_1$ and $\alpha_2 > \mu_2$), because all eigenvalues become negative.

The non-trivial equilibrium point $\bar{Q}^c$, with coordinates given in equation (9), has one of them zero ($\bar{C} = 0$). The eigenvalues corresponding to the trivial equilibrium point $\bar{Q}^c$ are obtained from the Jacobian $\bar{J}^c$. Once $\bar{C} = 0$, one of the eigenvalues is $\lambda_1 = -\beta_1(\bar{T} - T_C)$, arising one of the conditions to the not real cancer equilibrium $\bar{Q}^c$ being stable, that is, $\bar{T} > T_C$, where T_C is given by equation (7). The remaining four eigenvalues are obtained from the sub-matrix $\bar{J}_1^c$, which comes from $\bar{J}^c$ excluding first row and first column. Let us define matrix A as $A = -\bar{J}_1^c$, or,

$$A = \begin{bmatrix} \frac{\alpha_2}{k_2}\bar{E} & \gamma\bar{E} & 0 & 0 \\ 0 & \frac{\alpha_3}{k_3}\bar{A}\bar{T} & 0 & -j_1 \\ -\gamma\bar{T} & -\gamma\bar{E} & j_2 & 0 \\ 0 & -j_3 & -\delta & j_4 \end{bmatrix}, \tag{14}$$

where j_1, j_2, j_3 and j_4 were defined in equation (13). In appendix B we show that, for big solution $T_>$, A is an M-matrix, and, hence, all eigenvalues associated to $\bar{J}_1^c$ have negative real part. Hence, $\bar{Q}^c$, which is biologically feasible but not real cancer, is locally asymptotically stable only if $\bar{T} > T_C$. Therefore, $\bar{Q}^c$ appears when one of the constraints to $\bar{Q}^*$ be biologically feasible is violated: in the equation (4), instead of $\bar{C} < 0$, we have $\bar{C} = 0$ for $\beta_1 \geq \beta_1^c$.

The local stability of the non-trivial equilibrium $\bar{Q}^*$ is performed numerically. However, we stress the fact that the equilibrium $\bar{Q}^c$ is an extension of $\bar{Q}^*$ for $\beta_1 \geq \beta_1^c$. Hence, the big solution $T_>$of equation (5) for $\beta_1 \geq \beta_1^c$ must be stable. For this reason we showed the local stability of $\bar{Q}^c$, even though this is not a real cancer equilibrium.

Results and Discussion

In this section we present numerical simulations of the model, which are discussed. The numerical methods used are bisection (to find zeros of polynomials) and 4^{th} order Runge-Kutta (to solve system of ordinary differential equations) [16].

Numerical analysis of the model

Numerical simulations are performed taking into account the values and units of the model's parameters given in Table 2. These values have the purpose of illustrating the outcomes of the model. Cancer free equilibrium point $\bar{Q}^0$ has the cancer free concentrations: $C_0 = 9$ *cells/uv* and $E_0 = 10$ *cells/uv*, where *uv* stands for an arbitrarily unit of volume. Hereafter we will omit units of all variables and parameters. In this section we deal with the steady state of the system (1), determining the equilibrium points and bifurcation diagrams. We also study the dynamical trajectories of the system (1) assuming that mutations occurred and cancer cells arise suddenly. For this reason the initial conditions are given by equation (2). The reason behind this is the fact that the trivial equilibrium point $\bar{Q}^0$ always exists and is stable. Hence, the initial conditions

Table 2 Values of the parameters

Parameters	Fixed values	Alternative values**	Units
α_1	0.1		$days^{-1}$
α_2	0.1		$days^{-1}$
α_3	0.2	5.0	$[A]^{-1} \times days^{-1}$
ε	0.01*	0.1	$[T]^{-1} \times days^{-1}$
μ_1	0.01		$days^{-1}$
μ_2	0.05		$days^{-1}$
μ_3	0.05	0.005	$days^{-1}$
μ_4	0.01		$days^{-1}$
μ_5	0.01		$days^{-1}$
k_1	10		$[C]$
k_2	20		$[E]$
k_3	5	0.1	$[T]$
k_4	1	0.2	$[A]$
δ	0.1		$days^{-1}$
γ	0.01*	0.02	$[T]^{-1} \times days^{-1}$
β_1	0.01*		$[T]^{-1} \times days^{-1}$
β_2	0.01*		$[C]^{-1} \times days^{-1}$

The values for model's parameters. The unity of [•] is number of cells of type • per unit of volume, *•/uv*. Parameters regarded to the non-linear terms of the dynamical system are allowed to vary (indicated by the symbol*). The values of the parameters that differ from the fixed values are in the column indicated with **.

supplied to the system of equations correspond to an appearance of C_m number of cancer cells in a cancer free situation $\bar{Q}^0$, that is, at time $t = 0$ the variables assume $C(0) = C_0 - C_m$, $E(0) = E_0$, $T(0) = C_m$, $P(0) = 0$ and $A(0) = 0$. The initial amount of cancer cells is originated by mutation from several sources. In some special situations we will use $C(0) = C_0$. The initial amount of mutations C_m can either grow up to cancer, or fades out.

Based on the values given in Table 2, the constraints, using equations (7) and (8), are $T_C = 9.0$ (at $\beta_1 = 0.01$), $T_E = 5.0$, $T_A = 5.0$ and $T_g = 14.0$. The coordinates of the non-trivial equilibrium points, corresponding to small ($T_<$) and big ($T_>$) equilibrium values of cancer cells obtained from equation (5), are, respectively, $\bar{Q}^*_< = (8.92, 9.85, 0.08, 0.07, 0.71)$ and $\bar{Q}^*_> = (5.32, 2.64, 3.68, 0.88, 1.96)$, from equation (4). The corresponding five eigenvalues (λ_i, $i = 1, ..., 5$) are given in Table 3, showing that the small is unstable ($\lambda_1 > 0$), while the big is stable (all λ_i's are negative). The big equilibrium $T_> = 3.68$ satisfies the constraints given in equation (7). The trivial equilibrium $\bar{Q}^0$ is always stable.

In Figure 1 we illustrate the dynamical trajectories of system (1) taking into account the values of parameters given in Table 2. The dynamical trajectories depend on the

Table 3 Eigenvalues

Eigenvalues	Corresponding to $Q^*_<$	Corresponding to $Q^*_>$
λ_1	+0.028	-0.227 - *i*0.024
λ_2	-0.089 - *i*0.060	-0.227+ *i*0.024
λ_3	-0.089 + *i*0.060	-0.068
λ_4	-0.064	-0.0293 - *i*0.0059
λ_5	-0.047	-0.0293 + *i*0.0059

Eigenvalues (λ_i, $i = 1,..., 5$) corresponding to the non-trivial equilibrium points $\bar{Q}^*_<$ (unstable) and $\bar{Q}^*_>$ (stable) using values given in Table 2.

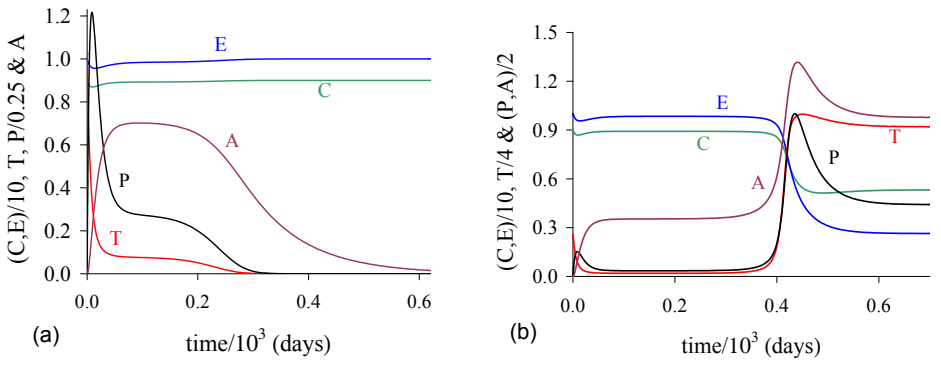

Figure 1 Dynamical trajectories using values in Table 2. Dynamical trajectories of the system (1) considering the values of parameters given in Table 2. The initial conditions determine the region of attraction: trivial $\bar{Q}^0$ for $T(0)$ = 1.023 (a), or non-trivial $\bar{Q}^*_>$ (b). The scales of vertical and horizontal axes must be multiplied by the factors shown in the legends to obtain the actual values.

initial conditions. In Figure 1(a), due to $T(0)$ = 1.023, the dynamical trajectories are attracted to the trivial equilibrium $\bar{Q}^0$; while for $T(0)$ = 1.024, the dynamical trajectories attain the non-trivial equilibrium $\bar{Q}^*_>$ (Figure 1(b), which shows a sudden relapse to cancer onset at around 400 *days*). The exact critical amount of cancer cells T^* that divides two regions of attraction situates in the open interval (1.023,1.024). Notice that T^* is much higher than $T_<$= 0.08, which comes out due to other initial conditions. However, if the initial conditions are the coordinates of $\bar{Q}^*_<$, except $T(0)$, that is, $C(0)$ = 8.92, $E(0)$ = 9.85, $P(0)$ = 0.07 and $A(0)$ = 0.71, then, for an arbitrary value $\epsilon > 0$, the dynamical trajectories go to trivial $\bar{Q}^0$ when $T(0) = (1 - \epsilon) \times 0.08$, and to the non-trivial $\bar{Q}^*_>$ when $T(0) = (1 + \epsilon) \times 0.08$ (for instance, ϵ = 0.001, figures not shown). In this case, we have $T^* = T_<$. Hence, $\bar{Q}^*_<$ is the break-point, and its coordinates generate a hyper-surface that divides two attracting regions (see Appendix A). Notice that $T(0)$ = 1.023 which plays the role of separating two attracting regions is 12-fold higher than $T_<$= 0.08.

The initial amount of normal cells that suffer mutation C_m is crucial to trigger cancer disease. Figure 1 shows that if this amount is below a critical value, that is, $T(0) = C_m < T^*$, then repairing systems act efficiently and cancer does not settle in an organ. However, if the mutated cells surpass the critical value, the repairing systems do not avoid the onset of cancer.

Next, numerical simulations are performed in order to assess the effects of varying parameters β_1, β_2, γ and ε. In all dynamical trajectories, remember that unstable solution $T_<$is very small, but $T(0)$ is higher due to the initial conditions supplied to system (1) correspond to the coordinates of the trivial equilibrium $\bar{Q}^0$, and not those of the unstable $\bar{Q}^*_<$. Hence, $T(0)$ is not comparable with $T_<$, one of the coordinates of the break-point $\bar{Q}^*_<$. The cancer cells proliferate above the subclinical threshold of 10^3 cells and reach 10^9 cells which is the X-ray detectable threshold [11].

Interaction between normal and cancer cells - β_1 and β_2

Direct competition between normal and cancer cells for resources and space occur in order to grow. But there are many factors that affects both populations, like indirect

interaction as excretion released by cells, changes in the environment and control mechanisms. The parameters β_1 and β_2 take into account these factors also.

Let us assess the cancer cells affecting negatively in the normal cells, by varying β_1.

In Figure 2 we show $\bar{T}$, the solutions of $f(T)$ - $g(T)$ = 0. Figure 2(a), which corresponds to the figure shown in Appendix A with $T_E = T_A = 5.0$, shows the existence of two positive solutions: small (denoted by $T_<$) and big (denoted by $T_>$) for four values of β_1: 0.01 (labelled b_1), 0.1 (b_2), 1.0 (b_3) and 10.0 (b_4). In Figure 2(b) a zoom near lower values of β_1 is shown to enhance the small solution $T_<$.

Let us vary β_1 and compute the corresponding equilibrium value $\bar{T}$ using equation (5). As shown in Figure 2, we have two positive solutions: small, $T_<$, and big, $T_>$. Substituting this solution into equation (4), we obtain the coordinates of the non-trivial equilibrium point $\bar{Q}^*$. In Figure 3 we show the coordinates of the equilibrium points $\bar{Q}^*_<$ (a) and $\bar{Q}^*_>$ (b). In (b) we also show the curves of T_C and T_g, which intercept the curve of big solution $T_>$. When $T_>= T_C$, which occurs at $\beta_1 = \beta_1^c = 2.1273 \times 10^{-2}$, we have $\bar{C} = 0$, at which the big non-trivial $\bar{Q}^*_>$ disappears and arises an another equilibrium $\bar{Q}^c_>$, with $\bar{C} = 0$ and other coordinates given by equation (9), which has fixed value $T_> = T_C^c = (\alpha_1 - \mu_1)/\beta_1^c = 4.2306$ for $\beta_1 \geq \beta_1^c$. Coordinates of $\bar{Q}^c_>$ are same for all $\beta_1 \geq \beta_1^c$. Mathematically, there is another value of β_1, which does not change the existing equilibrium point $\bar{Q}^c$, at which we have $T_>= T_g$, that is, $\beta_1 = \beta_1^A = 2.8001 \times 10^{-2}$. At this value we have $\bar{A} = 0$, with $T_> = T_g^A = \dfrac{\alpha_1\mu_3}{\beta_1^A\beta_2 k_1} + \dfrac{\alpha_1 - \mu_1}{\beta_1^A} = 4.9996$.

Figure 3 shows that trivial $\bar{Q}^0$ and small non-trivial $\bar{Q}^*_<$ exist for all β_1, but big non-trivial is $\bar{Q}^*_>(\beta_1 < \beta_1^c)$ or $\bar{Q}^c_>(\beta_1 \geq \beta_1^c)$. In Figure 4, we show the bifurcation diagram, considering $\bar{T}$ as a function of β_1 (curve T in (a) and (b) of Figure 3). For all values of β_1 the small equilibrium point $\bar{Q}^*_<$ is the break-point, which divides two regions where trivial $\bar{Q}^0$ or big non-trivial $\bar{Q}^*_>$ (or $\bar{Q}^c_>$) is attracting point. Initial conditions set in a small region marked with I and Ia are attracted to the trivial equilibrium point $\bar{Q}^0$.

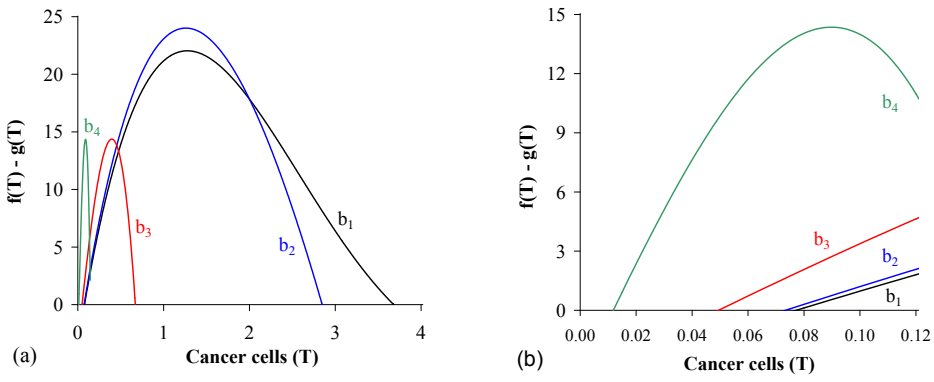

Figure 2 Two Positive solutions for four values of β_1. Two positive roots for the equation $f(T) = g(T)$, for four values of β_1. In (a) we show both roots, while in (b), a zoom near lower values of β_1. Legends of curves stand for: b_1 = 0.01 (Table 2), b_2 = 0.1, b_3 = 1.0 and b_4 = 10.0.

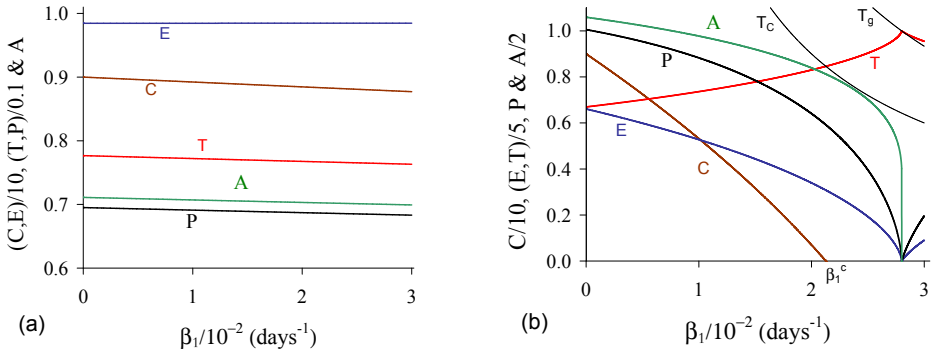

Figure 3 Positive equilibrium values varying β_1. The coordinates of the positive equilibrium points varying β_1. In (a) we show the coordinates of the small equilibrium point $\bar{Q}^*_<$, and in (b), of the big equilibrium point $\bar{Q}^*_>$. The coordinates of $\bar{Q}^*_<$ is quite insensitive with variation in β_1, and in (b) we also show the curves of T_C ($\bar{C} = 0$ at $\bar{T} = T_C$) and T_g ($\bar{A} = 0$ at $\bar{T} = T_g$). The small root $T_<$decreases very slowly, while the big one $T_>$ increases up to $T_> = T_g$, and then, decreases. The scales of vertical and horizontal axes must be multiplied by the factors shown in the legends to obtain the actual values.

However, initial conditions set in regions marked with II and III are attracted to big non-trivial equilibrium point $\bar{Q}^*_>$ for $\beta_1 < \beta_1^c$, while for $\beta_1 \geq \beta_1^c$ (regions marked with IIa and IIIa), to $\bar{Q}^c_>$. Notice that $T_<$always decreases very slowly with β_1 (see also Figure 3(a)), showing that as β_1 increases, less amount of initial cancer cells is needed to trigger a cancer. But this variation is quite insensitive.

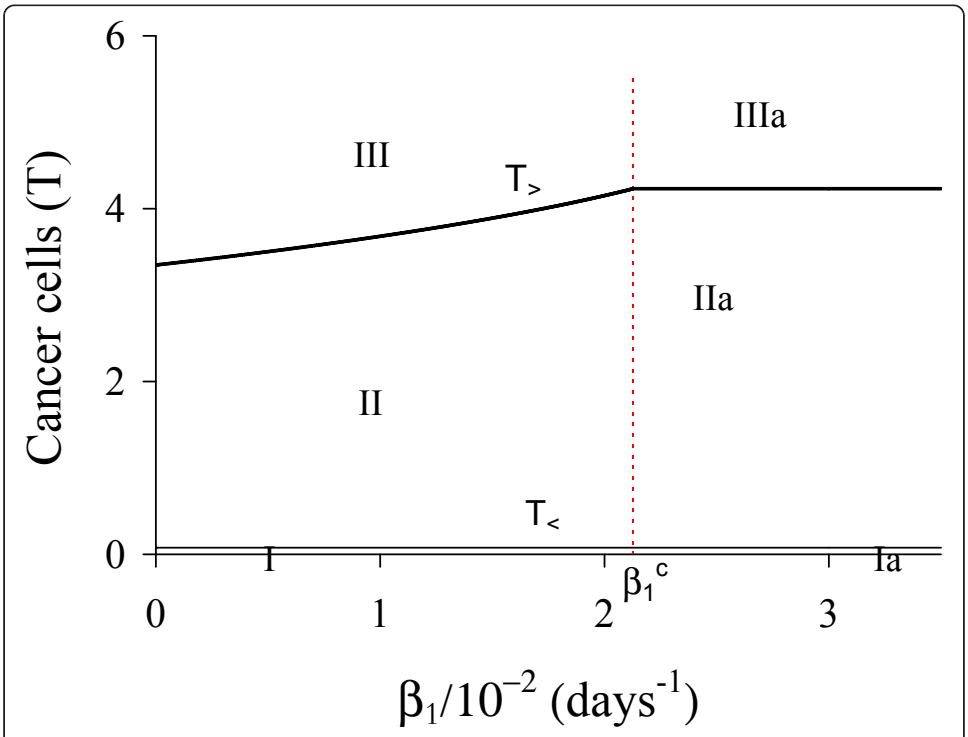

Figure 4 Bifurcation diagram varying β_1. The bifurcation diagram of $\bar{T}$ varying β_1, showing the attracting regions. With respect to the coordinates of small equilibrium point $\bar{Q}^*_<$ for all β_1, the trivial $\bar{Q}^0$ is attractor for initial conditions in a very small region I (and Ia). Initial conditions in regions II and III are attracted to $\bar{Q}^*_>$ for $\beta_1 < \beta_1^c$, and initial conditions in regions IIa and IIIa are attracted to $\bar{Q}^c_>$ for $\beta_1 \geq \beta_1^c$. The scales of vertical and horizontal axes must be multiplied by the factors shown in the legends to obtain the actual values.

In Figure 5 we show the dynamical trajectories, changing only β_1 in 1000 times the values of parameters given in Table 2, or β_1 = 10.0, being attracted to the special equilibrium point $\bar{Q}^c$, which is biologically feasible, but does not describe evolution of cancer. Dynamical trajectories are attracted to $\bar{Q}^0$ (a) when $T(0)$ = 0.151, while for $T(0)$ = 0.152, to $\bar{Q}^c_>$ (b). The dynamical trajectories in Figure 5 are similar to Figure 1, except C, which decreases abruptly to zero and situates practically in the vertical axis, and after 650 *days* increases quickly to $\bar{C}$ (a), or remains in the horizontal axis (b). Increasing β_1 in 100-fold, $T(0)$ decreased 7-fold. For another β_1 = 100.0, when $T(0)$ = 0.142, trajectories go to $\bar{Q}^0$; while for $T(0)$ = 0.143, to $\bar{Q}^c_>$, which coordinates have exactly the same values found in the previous case (β_1 = 10.0). Both cases (figures not shown) correspond to $\beta_1 > \beta_1^c$, hence $\bar{Q}^c_>$ are the same, while $\bar{Q}^c_<$ decrease little bit.

Let us assess the normal cells affecting negatively in the cancer cells, by varying β_2.

In Figure 6 we show the coordinates of the equilibrium points $\bar{Q}^*_<$ (a) and $\bar{Q}^*_>$ (b) by varying β_2. Positive solutions for equation (5) disappeared for higher β_2.

In Figure 7, we show the bifurcation diagram, considering $\bar{T}$ as a function of β_2 (curve T in (a) and (b) of Figure 6). For $\beta_2 < \beta_2^{th}$, initial conditions set in region marked with I are attracted to the trivial equilibrium point $\bar{Q}^0$, while for those set in regions II and III are attracted to big non-trivial equilibrium point $\bar{Q}^*_>$. However, for $\beta_2 > \beta_2^{th}$ all initial conditions are attracted to $\bar{Q}^0$, which is the unique equilibrium, because there is not any positive solution for equation (5). Hence, there is a threshold of the parameter β_2, denoted by β_2^{th}, above which all trajectories go to trivial equilibrium. At the threshold value $\beta_2^{th} = 4.8376 \times 10^{-2}$ both roots assume same value, that is, $T_<(\beta_2^{th}) = T_>(\beta_2^{th}) = 0.7053$.

For $\beta_2 < \beta_2^{th}$ the dynamical trajectories are similar to that shown in Figure 1. For instance, when β_2 = 0.04, for $T(0)$ = 10.60 trajectories are attracted to $\bar{Q}^0$; while for $T(0)$ = 10.61, to $\bar{Q}^*_>$. Notice that increasing β_2 in 4-fold, $T(0)$ increased 10-fold, showing

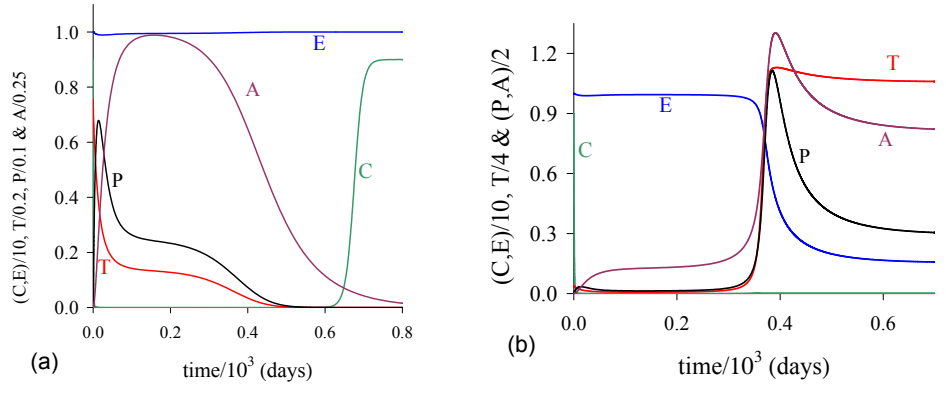

Figure 5 Dynamical trajectories using β_1 = 10.0. Dynamical trajectories of the system (1) considering the values of parameters given in Table 2, except β_1 = 10.0. The initial conditions determine the region of attraction: trivial $\bar{Q}^0$ for $T(0)$ = 0.151 (a), or non-trivial $\bar{Q}^*_>$ for $T(0)$ = 0.152 (b). The scales of vertical and horizontal axes must be multiplied by the factors shown in the legends to obtain the actual values.

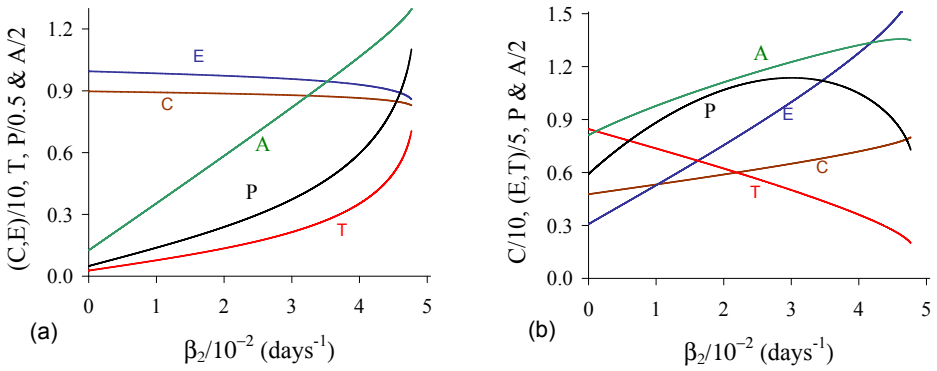

Figure 6 Positive equilibrium varying β_2. The coordinates of the positive equilibrium points varying β_2. In (a) we show the coordinates of the small equilibrium point $\bar{Q}^*_<$, and in (b), of the big equilibrium point $\bar{Q}^*_>$. The small root $T_<$increases, while the big one $T_>$ decreases up to β_2^c, at which $T_<= T_<$, and then $f(T) = g(T)$ does not have positive solution. The scales of vertical and horizontal axes must be multiplied by the factors shown in the legends to obtain the actual values.

that negative influence on cancer cells by normal cells affects strongly (very sensitive) in the cancer dynamics. For $\beta_2 > \beta_2^{th}$, all initial conditions are attracted to trivial disregarding initial conditions. Figure 8 shows an extreme example, changing only β_2 in 100 times the values of parameters given in Table 2, or β_2 = 1.0. In this simulation we consider a very high (unrealistic) initial conditions $T(0)$ = 100.0, even though $\bar{Q}^0$ is the

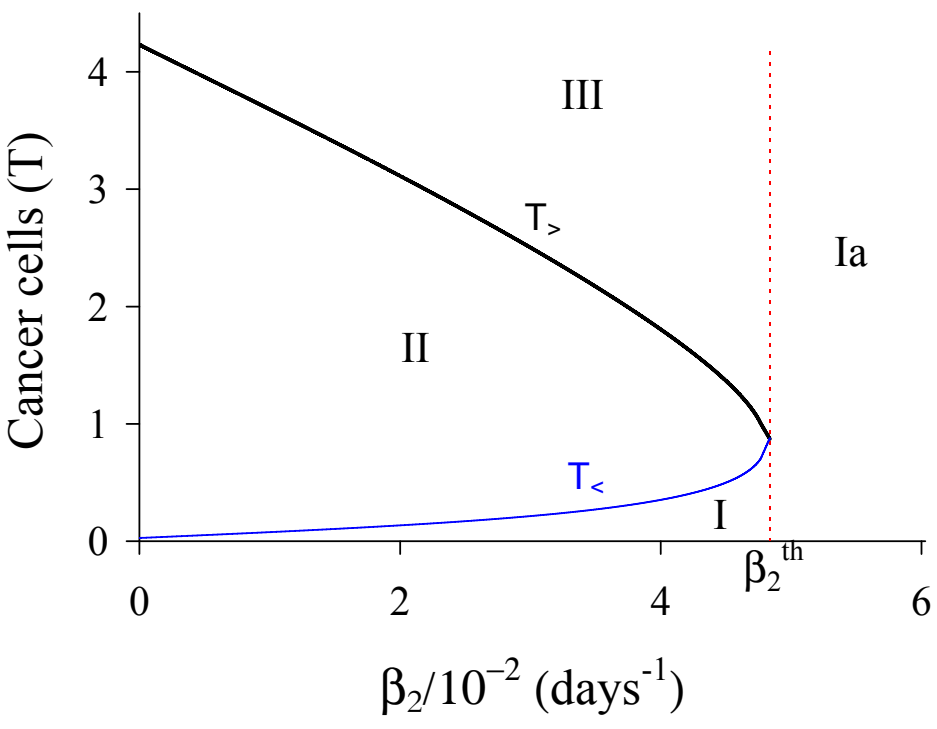

Figure 7 Bifurcation diagram varying β_2. The bifurcation diagram of $\bar{T}$ varying β_2, showing the attracting regions. With respect to the coordinates of small equilibrium point $\bar{Q}^*_<$ for $\beta_2 < \beta_2^{th}$, the trivial $\bar{Q}^0$ is attractor for initial conditions in region I, and for regions II and III, trajectories are attracted to $\bar{Q}^*_>$. For $\beta_2 > \beta_2^{th}$, all initial conditions (region Ia) are attracted to $\bar{Q}^0$. The scales of vertical and horizontal axes must be multiplied by the factors shown in the legends to obtain the actual values.

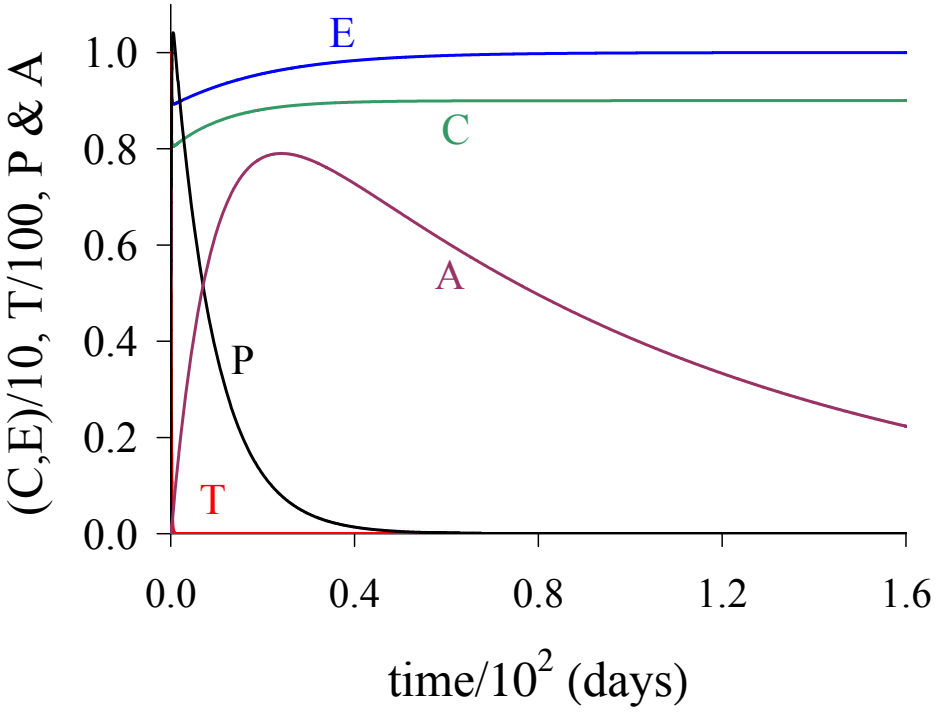

Figure 8 Dynamical trajectories using β_2 = 0.04. Dynamical trajectories of the system (1) considering the values of parameters given in Table 2, except β_2 = 0.04 (near β_2^{th}). The initial conditions determine the region of attraction: trivial $\bar{Q}^0$ for $T(0)$ = 10.60 (a), or non-trivial $\bar{Q}^*_>$ for $T(0)$ = 10.61 (b). The scales of vertical and horizontal axes must be multiplied by the factors shown in the legends to obtain the actual values.

attractor: we observe that T decreases quickly (practically in the vertical axis), and A decreases slowly. We stress the fact that we used as the initial condition for C, the equilibrium value of normal cells, that is, $C(0) = C_0 = 9.0$, because the amount C_m in the initial condition for T is higher than C_0.

As β_1 increases, the initial number of cancer cells (for instance, originated by mutation) needed to trigger a cancer $T(0) = C_m$ is decreased, but smoothly. Also, the normal cells can be displaced by cancer cells for values of β_1 higher than its critical value, that is, $\beta_1 > \beta_1^c$. With respect to β_2, we observed a threshold for β_2, β_2^{th}, above which cancer can not be settled. Also, as β_2 increases, the initial number of cancer cells needed to trigger a cancer C_m increases quickly, avoiding the process of cancer disease. Therefore, cancer can be settled in an organ if the following combination matches: better fitness of cancer cells (β_1 increases), and decrease in the efficiency of the repairing systems (β_2 decreases).

Recruitment of existing epithelial cells - γ

New network of blood vessels is created by cancer cells to provide nutrients and oxygen to support their growth. This new network depends on the capacity of originating sprouts from the existing blood vessel network, and is described by the parameter γ, which is varied.

In Figure 9 we show the coordinates of the equilibrium points $\bar{Q}^*_<$ (a) and $\bar{Q}^*_>$ (b) by varying γ. The small $T_<$decreases, while the big $T_>$decreases after an initial increase. Notice that $T_>$decreases due to the fact that pre-existing blood vessels E decreases

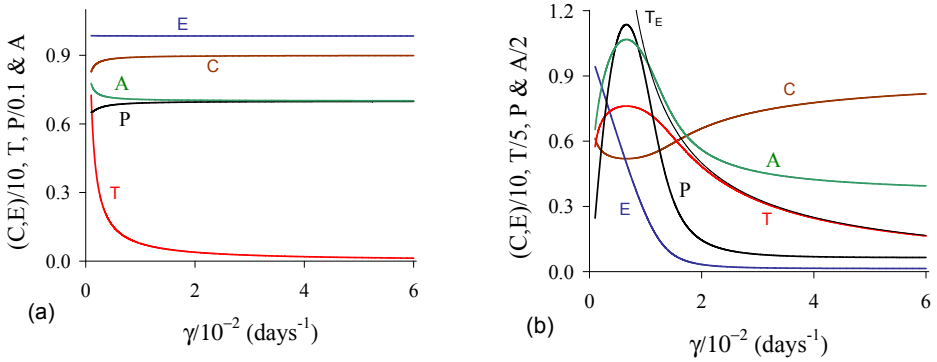

Figure 9 Positive equilibrium values varying γ. The coordinates of the positive equilibrium points varying γ. In (a) we show the coordinates of the small equilibrium point $\bar{Q}^*_<$, and in (b), of the big equilibrium point $\bar{Q}^*_>$. In (b) we also show the curve of T_E, which is always greater than $T_>$. The small root $T_<$decreases, while the big one $T_>$ decreases after an initial increase. The scales of vertical and horizontal axes must be multiplied by the factors shown in the legends to obtain the actual values.

quickly. The new blood vessels A also decrease. The maximum of the variables occurs at around $\gamma = 6.57 \times 10^{-3}$ (for C is minimum). In Figure 9(b) we show the curve T_E, which depends on γ and situates always above the equilibrium value $T_>$. Hence, we have non-trivial equilibrium point $\bar{Q}^*$ for sufficiently higher values of γ.

In Figure 10, we show the bifurcation diagram, considering $\bar{T}$ as a function of γ (curve T in (a) and (b) of Figure 9, which appear at $\gamma = \gamma^{th}$). In (b), a zoom near zero is shown. In Figures 10(a) and 10(b), for $\gamma > \gamma^{th}$ initial conditions set in regions marked with I, Ia and Ib are attracted to the trivial equilibrium point $\bar{Q}^0$. However, initial conditions set in regions marked with II and III are attracted to $\bar{Q}^*_>(\gamma^{th} < \gamma < \gamma_1^c)$; to a limit cycle circulating $\bar{Q}^*_>$ in regions IIa and IIIa $(\gamma_1^c < \gamma < \gamma_2^c)$; and to $\bar{Q}^0$ in regions IV and V $(\gamma > \gamma_2^c)$, where E decreases and, then, increases to equilibrium value E_0.

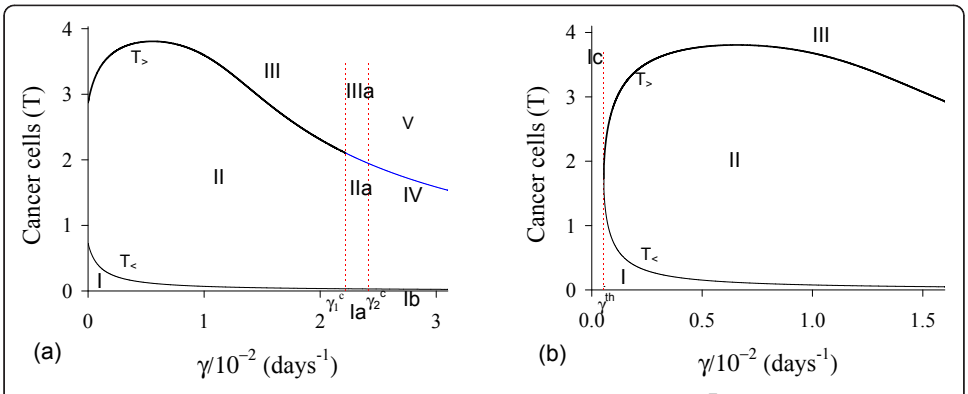

Figure 10 Bifurcation diagram varying γ. The bifurcation diagram of $\bar{T}$ varying γ, showing the attracting regions. In (a) we show wide range of variation of γ, and in (b), a zoom near origin. For $\gamma < \gamma^{th}$ (b) the trivial $\bar{Q}^0$ is attractor for all initial conditions (region Ic). For $\gamma > \gamma^{th}$ (a), with respect to the coordinates of small equilibrium point $\bar{Q}^*_<$, the trivial $\bar{Q}^0$ is attractor for regions I, Ia and Ib; and we have three possibilities: (1) for $\gamma^{th} < \gamma < \gamma_1^c$, the non-trivial $\bar{Q}^*_>$ is attractor for initial conditions in regions II and III; (2) for $\gamma_1^c < \gamma < \gamma_2^c$, stable limit cycle circulating unstable $\bar{Q}^*_>$, in regions IIa and IIIa; and (3) for $\gamma > \gamma_2^c$, trivial $\bar{Q}^0$ is attractor for regions IV and V. In the latter case, the way to reaching the trivial equilibrium is different for initial conditions in Ib and IV or V. The scales of vertical and horizontal axes must be multiplied by the factors shown in the legends to obtain the actual values.

The Hopf bifurcation occurs at $\gamma = \gamma_1^c$ (supercritical) and $\gamma = \gamma_2^c$ (subcritical) [17]. The special values are: $\gamma^{th} = 5.450 \times 10^{-4}$ and $T_>(\gamma^{th}) = 1.74$, $\gamma_1^c = 2.3196 \times 10^{-2}$ and $T_>(\gamma_1^c) = 2.1029$, and $\gamma_2^c = 2.5161 \times 10^{-2}$ and $T_>(\gamma_2^c) = 1.9443$. Figure 9(b) showed that at $\gamma \simeq \gamma_1^c$, E is very low. For $\gamma < \gamma^{th}$ (b), all initial conditions set in region marked with Ic are attracted to the trivial equilibrium point $\bar{Q}^0$, which is the unique equilibrium, because there is not any positive solution for equation (5). Hence, there is a threshold of the parameter γ, denoted γ^{th}, below which all trajectories go to trivial equilibrium.

In cancer disease, it is expected that a small number of epithelial cells must be recruited in order to build up new vascularization from the sproutings. For small values of γ but higher than the threshold ($\gamma > \gamma^{th}$), the dynamical trajectories follow those shown in Figure 1. In Appendix C we illustrate the Hopf bifurcation, which behavior is not compatible with real cancer. Considering number of tumor cells, concentration of growth factor and volume of blood vessels feeding the tumor, Agur *et al*. [18] showed that Hopf bifurcation can not occur if ordinary differential equations are used. But, Hopf bifurcation can occur if time-delay is encompassed. Our model presented Hopf bifurcation, however only in a range of values of parameter γ which is not compatible with biological findings.

Solid tumors need extra source of resources to attend the quick growth of cancer cells. Hence, cancer can be settled in an organ if the capacity of sprouting from existing vascularization is sufficiently higher ($\gamma > \gamma^{th}$). However, it must not be so higher in order to avoid the death of the cancer diseased person due to normal cells being displaced by cancer cells quickly.

Capacity of building up new vascularization - ε

The appearance of shunts from existing blood vessels to initiate new vascularizations was described by the parameter γ. New network of blood vessels is created by cancer cells to provide nutrients and oxygen to support their growth. After a period of time δ^{-1}, new vessels are built up from the shunts. The capacity of mounting up new vessels by cancer cells is analyzed by varying ε.

In Figure 11 we show the coordinates of the equilibrium points $\bar{Q}^*_<$ (a) and $\bar{Q}^*_>$ (b) by varying ε. Both small $T_<$and big $T_>$decrease. In (b), due to the solution $T_>(\varepsilon = 0) = 5.0$, we used equation (12) for $f(T)$ and $g(T)$ to obtain $\bar{A}(0) = 4.457$.

In Figure 12, we show the bifurcation diagram, considering $\bar{T}$ as a function of ε (curve T in (a) and (b) of Figure 11). When $\gamma > 0$, there are not neither special nor threshold values: when initial conditions are set in a small region I, trajectories are attracted to the trivial equilibrium point $\bar{Q}^0$, and for initial conditions set in regions II and III, trajectories are attracted to $\bar{Q}^*_>$ (a). This behavior results by the existence of influx in equation for A, given by the term γP. Hence, if we let $\gamma = 0$, a different bifurcation arises (b).

There is a threshold of ε, denoted ε^{th}, below which all trajectories go to trivial equilibrium. For $\varepsilon > \varepsilon^{th}$, where $\varepsilon^{th} = 5.250 \times 10\text{-}^2$, we have similar behavior than that observed in (a), but $T_>$is increasing. In Figure 13 we show the dynamical trajectories depending on the initial conditions for $\gamma = 0$, changing only ε in 100 times the values of parameters given in Table 2, or $\varepsilon = 1.0$. Dynamical trajectories are attracted to $\bar{Q}^0$

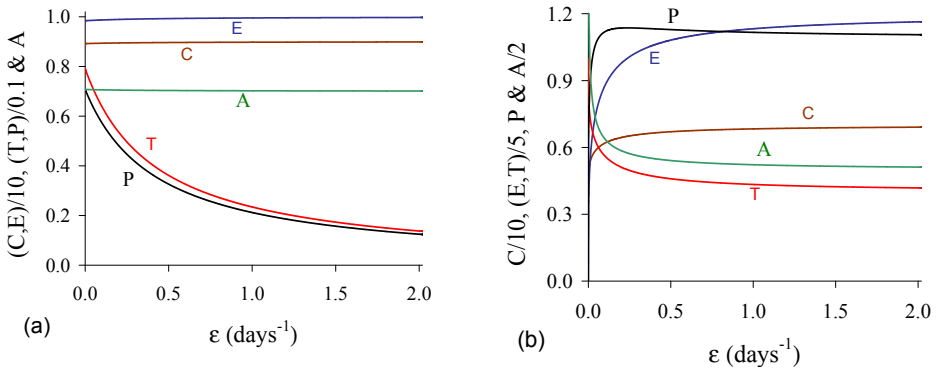

Figure 11 Positive equilibrium values varying ε. The coordinates of the positive equilibrium points varying ε. In (a) we show the coordinates of the small equilibrium point $\bar{Q}^*_<$, and in (b), of the big equilibrium point $\bar{Q}^*_>$. The coordinates of $\bar{Q}^*_<$ and $\bar{Q}^*_>$ decrease. The scales of vertical and horizontal axes must be multiplied by the factors shown in the legends to obtain the actual values.

(a) when $T(0) = 0.416$, while for $T(0) = 0.417$, to $\bar{Q}^*_>$ (b). The dynamical trajectories in (a) are similar to Figure 1(a). Increasing ε in 100-fold, $T(0)$ decreased 2.5-fold.

Due to the influx γP, which is a linear term, in the equation for A, the parameter ε that describes the mounting up of new vascularization does not present any special behavior, except by the dependency with the initial conditions. However, when $\gamma = 0$, there arises a threshold of ε, called ε^{th}, above which new vascularizations promoted by cancer cells can occur. The case $\gamma = 0$ means that cancer cells are supported exclusively by the new network of blood vessels originated from surrounding tissues for instance, and the pre-existing one maintains its function of nourishing exclusively the normal cells.

Angiogenesis is the process by which new blood vessels develop from an existing vasculature, through endothelial cell sprouting, proliferation, and fusion. Hence,

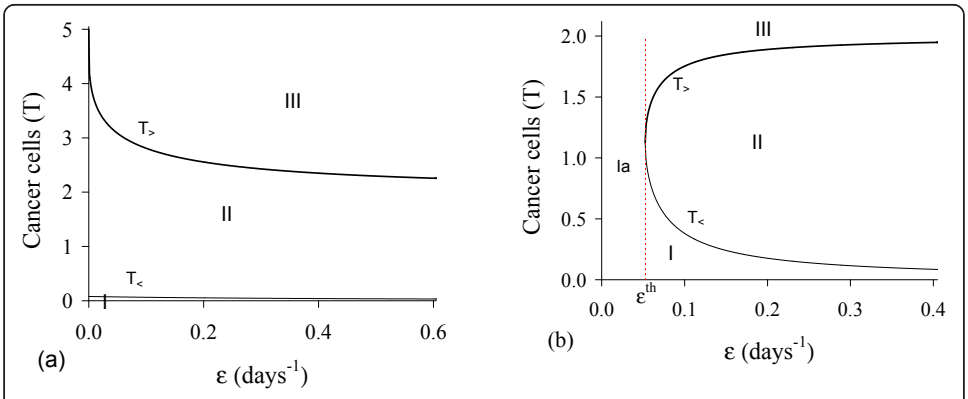

Figure 12 Bifurcation diagram varying ε. The bifurcation diagram of $\bar{T}$ varying ε, showing the attracting regions. With respect to the coordinates of small equilibrium point $\bar{Q}^*_<$, the trivial $\bar{Q}^0$ is attractor for initial conditions in a very small region I, and for initial conditions in regions II and III $\bar{Q}^*_>$ is the attractor (a). There is not a critical value due to influx γP in equation for A. However, for $\gamma = 0$, we have bifurcation diagram similar to the Figure 10.b: for $\varepsilon < \varepsilon^{th}$, trivial $\bar{Q}^0$ is attractor in I (and for all initial conditions in Ia), and $\bar{Q}^*_>$ is attractor in II and III (b) for $\varepsilon > \varepsilon^{th}$. The scales of vertical and horizontal axes must be multiplied by the factors shown in the legends to obtain the actual values.

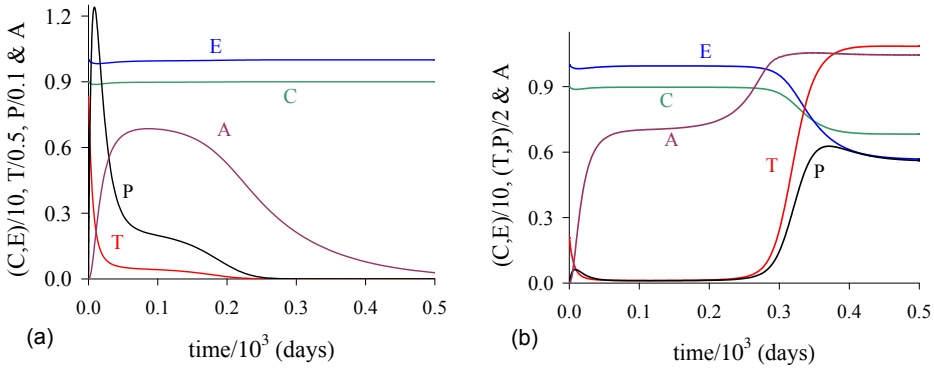

Figure 13 Dynamical trajectories using $\varepsilon = 1.0$. Dynamical trajectories of the system (1) considering the values of parameters given in Table 2, except $\varepsilon = 1.0$. The initial conditions determine the region of attraction: trivial $\bar{Q}^0$ for $T(0) = 0.416$ (a), or non-trivial $\bar{Q}^*_>$ for $T(0) = 0.417$ (b). The scales of vertical and horizontal axes must be multiplied by the factors shown in the legends to obtain the actual values.

angiogenesis create new vascularization from sprouting originated in existing vasculature, which was called pre-angiogenesis. Due to the endothelial cell sprouting promoted by the vascular endothelial growth factor, cancer cells can grow even in the absence of new vascularization ($\varepsilon = 0$), being the size of cancer cells big with higher capacity of mounting up new vascularization (increasing ε).

Discussion

In foregoing section we have used for k_3 and k_4 values comparable to k_1 and k_2 in order to enhance the results. In other words, cancer related cells are allowed to grow comparable to the size of normal cells, which is not true. In real world, cancer related cells are found in much smaller size, hence k_3 and k_4 must be lower than k_1 and k_2, being the relative size depending on the organ of the body.

In Figure 14 we show dynamical trajectories using the initial conditions given in equation (2). The values of the parameters are given in the column marked with ** of Table 2, and other parameters are those given in fixed values. Dynamical trajectories

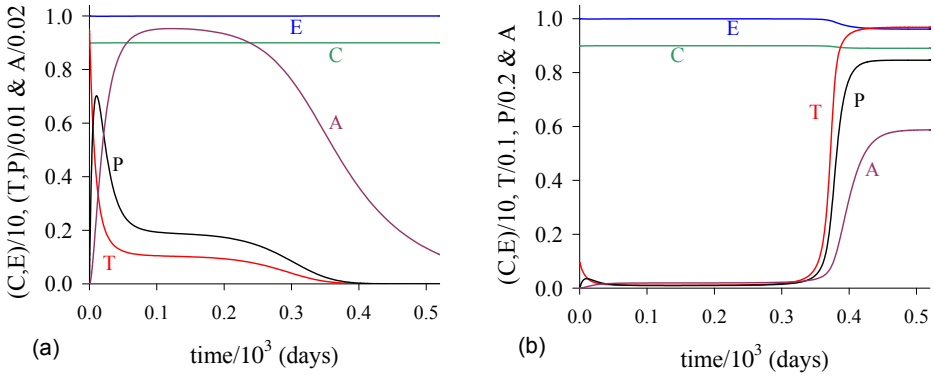

Figure 14 Dynamical trajectories using alternative values. Dynamical trajectories of the system (1) considering the fixed values of parameters given in Table 2, except those in the column marked with **. The initial conditions determine the region of attraction: trivial $\bar{Q}^0$ for $T(0) = 9.51 \times 10^{-3}$ (a), or non-trivial $\bar{Q}^*_>$ for $T(0) = 9.52 \times 10^{-3}$ (b). The scales of vertical and horizontal axes must be multiplied by the factors shown in the legends to obtain the actual values.

are attracted to $\bar{Q}^0$ (a) when $T(0) = 9.51 \times 10^{-3}$, while for $T(0) = 9.52 \times 10^{-3}$, to $\bar{Q}^*_>$ (b). The cancer is triggered at around 400 *days*. Decreasing k_3 in 50-fold (and some values of other parameters were also changed), the initial value that divides two attracting regions $T(0)$ is around 100-fold lower than that shown in Figure 1. In Figure 1, T reaches the asymptotic value near $k_3 = 5.0$, while in Figure 14, near $k_3 = 0.1$. Then all previous simulations can be translated to real world by appropriate scaling factors.

The initial amount of cancer cells originated from normal cells by mutations plays an important role in the dynamics of cancer growth. When the interacting parameters β_1, γ and ε increase, the small solution $T_<$decreases. This decrease in the initial cancer cells necessary to trigger the cancer is mediated by cancer cells that: (1) inhibit and occupy normal cells habitat (β_1); (2) produce higher amount of substances which cause new blood vessels to grow (γ); and (3) construct new blood networks to nourish themselves (ε). In opposite way, when the interacting parameter β_2 increases, the small solution $T_<$also increases. Hence, when normal cells inhibit the growth of cancer cells by many factors as better fitness, increasing repairing action, and induction of apoptosis, then the onset of cancer is avoided.

Another important aspect in the cancer growth is the appearance of thresholds. The interacting parameters β_2 and γ present threshold values, respectively, β_2^{th} and γ^{th}. Usually the systems that control the production of substances that induce the formation of new blood vessels to grow operate normally, which have as consequence that cancer cells are unable to recruit the blood to supply their need to continue to proliferate, and they fade out at this early stage. However, cancer cells may begin to produce substances which cause new blood vessels to grow. This phenomenon is characterized by the threshold of γ. The threshold of β_2 can be understood as the well functioning repairing mechanisms and the low fitness of cancer cells in comparison with normal cells. The threshold of ε arises only for $\gamma = 0$, which mimics cancer cells being nourished only by the new network of blood vessels originated from surrounding tissues by vasculogenesis [14].

There are also critical values for parameters β_1 and γ. Critical value for β_1 is a mathematical artefact, because it is meaningless biologically (in general k_3 is very low in comparison with constraint T_E). With respect to γ, there are two critical values, named γ_1^c and γ_2^c. When γ increases, the epithelial cells E decrease, and damped oscillations appear. When γ approaches to γ_1^c, the oscillations are less damped, and when surpasses γ_1^c, regular oscillations occur. However, the amplitude of regular oscillations increases as γ approaches to γ_2^c, resulting for lowest values of E, T and A reaching zero values (see figures in Appendix C). When the lowest values are incapable to trigger new burst of cancer cells, the oscillations cease and the trivial is the attractor. This occurs when γ surpasses γ_2^c. Again both γ_1^c and γ_2^c do not bear any biological meanings, because the cure of cancer is due to the elimination of pre-existing network of blood vessels. The biological meaningless sustained oscillations begin at $\gamma = \gamma_1^c$ (the supercritical Hopf bifurcation) and cease at $\gamma = \gamma_2^c$ (the subcritical Hopf bifurcation).

For instance, considering values of Table 2, the column with **, we observe the same behavior than that found in figures shown in Appendix C as γ increases: (1) damped oscillations around $\bar{Q}^*$ for $\gamma = 0.75$; (2) regular oscillations around $\bar{Q}^*$ in the interval

[0.76,0.80]; and (3) to the trivial equilibrium $\bar{Q}^0$ for $\gamma = 0.81$. In the region of limit cycle, we observed that: (1) C oscillates between (8.9, 9.0) for all γ; E, P and A oscillate between (0, M), where M increases as γ increases; and (3) T oscillates between (m,0.1), where m decreases as γ increases. When m becomes very small, there is not burst of cancer cells, limit cycle is destroyed, and cancer fades out for higher values of γ. Notice that the amplitude of oscillations of normal cells C is not affected, in opposite way of epithelial cells E which drops to near 0.

Agur *et al*. [18] showed that ordinary differential equations admit Hopf bifurcation if and only if at least one time-delay is introduced in the tumor growth modeling. They then concluded that an appropriate candidate for describing the cancer growth is the alternative that includes time-delays in the tumor proliferation or angiogenesis process. They also concluded that further mathematical research is warranted for exploring time-delays in the biologically realistic domains in the parameter spaces. Our model, however, showed Hopf bifurcation without time-delay (in fact, there is an elapse of time between pre-angiogenesis and angiogenesis cells), and sustained oscillations occur only in biologically not realistic domains in the parameter space.

When the initial conditions, especially $T(0) = C_m$, are such that the non-trivial equilibrium is attractor, the cancer cells reach the level $T_>$. C_m increases with increasing β_1, decreases with β_2 and ε. Cancer cells can grow and reach higher levels when they affect negatively normal cells (β_1), but reach lower levels when normal cells acts as a barrier against them (β_2). When γ varies, $T_>$increases in the initial phase (E decreases), and then decreases (E is practically zero). The parameter γ plays an equivalent role of β_1, but, restricted only to E, which decreases it dramatically. For lower γ, there is sufficient number of E to increase A, but epithelial cells are exhausted as γ increases, and A decreases (see equation (4)). Finally, $T_>$decreases with ε, which comes out due to relative higher value of γ. The behavior of ε is strongly dependent on γ due to the influx γP in equation for A: for lower γ (also $\gamma = 0$), $T_>$increases with ε (see Figure 12(b)).

We introduced in the model an intermediate phase between epithelial cells and angiogenesis cells. The purpose was to consider a delay in new blood vessel formation (angiogenesis) by the period of time δ^{-1}. This can be suppressed by letting $\delta \to \infty$. In Figure 15 we show dynamical trajectories using the initial conditions given in equation (2), and values of the parameters given in the column marked with ** of Table 2, and other parameters are those given in fixed values, except δ. Dynamical trajectories are attracted: (1) for $\delta = 0.001$, to $\bar{Q}^0$ (not shown) when $T(0) = 2.492 \times 10^{-1}$, while for $T(0) = 2.493 \times 10^{-1}$, to $\bar{Q}^*_>$ (a); and (2) for $\delta = 10.0$, to $\bar{Q}^0$ (not shown) when $T(0) = 6.608 \times 10^{-3}$, while for $T(0) = 6.609 \times 10^{-3}$, to $\bar{Q}^*_>$ (b). The cancer is triggered at around 900 and 360 *days*, respectively for $\delta = 0.001$ and 10.0. Including Figure 14(b), the cancer trigger is delayed and initial cancer formation due to mutation must be increased as δ decreases.

Conclusions

Many models [5][19] have already been proposed to describe cancer growth, and some of those models have explicitly considered the spatial dimension [20-22], which has been shown to play a key role in the understanding of various tumor growth processes. Other models considered computational approach [23,24]. Spatial and computational

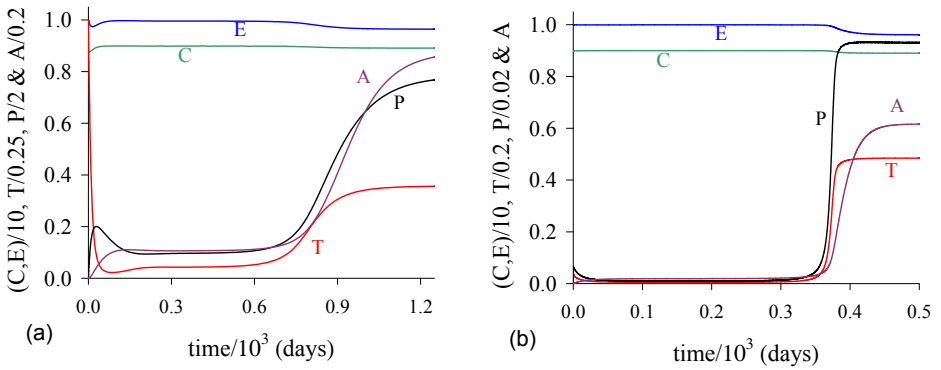

Figure 15 Dynamical trajectories using δ = 0.001 and δ = 10.0. Dynamical trajectories of the system (1) considering the fixed values of parameters given in Table 2, except those in the column marked with **. The initial conditions determine the region of attraction. For δ = 0.001 non-trivial $\bar{Q}^*$ is attractor when $T(0) = 2.493 \times 10^{-1}$ (a), while for δ = 10.0, when $T(0) = 6.609 \times 10^{-3}$ (b). The scales of vertical and horizontal axes must be multiplied by the factors shown in the legends to obtain the actual values.

modelings were analyzed numerically. However, we developed a zero-dimensional model for the initial stages of tumor angiogenetic growth in order to obtain analytical results.

In this model, various cell species are supposed to satisfy Lotka-Volterra growth laws. Neither metastasis nor geometry of the solid cancer were taken into account. The initial conditions (2), supplied to the dynamical systems (1), describe an impulsive system: in a steady state, a perturbation is introduced at a time $t = t_0 = 0$ as a form of pulse (Dirac delta function). This pulse mimics normal cells mutating to cancer cells. Cancer cells then promote the mounting of new network of blood vessels to nourish them after an elapse of time δ^{-1}. We introduced the pre-angiogenesis cells P to include the time delay in order to completing functional angiogenesis.

From the model, we conclude that the dynamical trajectories depend on the initial conditions supplied to the system, and also on interacting parameters. The cumulative effects of mutation is essential to originate a cancer cell. This effect is captured by the initial amount of cancer cells originating from normal cells, denoted by C_m. A sufficient number of cells must suffer mutation in order to a concentration of C_m cells really bear all necessary mutations to become effectively cancer cells. Our model is spatially homogeneous, hence the initial number of cancer cells is $C_m \times V$, where V is the volume of an organ of human body. In extremely favorable environmental and individual conditions, this initial number can be one.

Initially, cancer cells always can grow. But they fade out if they are unable to build up new blood vessels in order to supply their needs. The capacity of inducting new vascularization from existing blood vessel network must be efficient ($\gamma > \gamma^{th}$), and better fitness (increasing capacity of proliferation and capturing nutrients, decreasing mortality, etc.) of cancer cells (β_1 increases) in comparison with normal cells. Another aspect of cancer growth is corruption of the repairing systems, and in some extend we can think of that normal cells influencing negatively cancer cells play the role of repairing (fixing mutated DNA and inducting apoptosis). The parameter β_2 measures the efficient action of repairing system, and the effect of decreasing this value result in a higher level of corruption in the repairing system. Since cancer cells can recruit

epithelial cells to form new blood vessels, the capacity of proliferation of new vessels (ε) does not present threshold value.

The parameter γ can be thought of deviation of nutrients and oxygen from normal cells to feed cancer cells. This deviation does not affect normal cells because the carrying capacity of normal cells k_1 does not depend on the size of network of blood vessels. As γ increases, the deviated network plus the new one mounted by the action of angiogenesis effectors nourish the cancer cells. Hence, $\gamma = 0$ means that pre-existing network of blood vessels feeds normal cells, while the new network nourishes cancer cells. In this case, the capacity of cancer cells in promoting new vascularization is essential, which must surpass the threshold value ε^{th}. We obtained biologically feasible non-trivial equilibrium points, that is, the coordinates of the equilibrium points are positively defined. However, due to the simplifications assumed by model, the range of variations of parameters like β_1 and γ must be restricted. When $\beta_1 > \beta_1^c$ we have an equilibrium point $\bar{Q}^c$ with $\bar{C} = 0$, while for $\gamma_1^c < \gamma < \gamma_2^c$, we have limit cycle (sustained oscillations) with $E \sim 0$, but for $\gamma > \gamma_2^c$, we have abrupt increase of E, and the trivial equilibrium is attained. Both results can not be acceptable for cancer growth description.

Some results obtained here can be understood as vasculogenesis (when $\gamma = 0$) [14]. The dynamics of normal and cancer cells are similar than that presented in the model proposed by Nani and Freedman [11]. However, we did not take into account the action of immune system, while they did not take into account the angiogenesis. Agur *et al*. [18] proposed to examine the occurrence of Hopf bifurcation in the clinical context, that is, to check whether or not one can contain tumor growth by imposing time-delays in the processes of neo-vascularization. Our results showed that Hopf bifurcation occurs in biologically not realistic domains in the parameter space.

In a future work we will analyze a model in which the sizes of the normal and cancer cells are allowed to depend on the overall network of blood vessels: normal and cancer cells compete for nutrients provided by the pre-existing blood vessels, while cancer cells have additional source originated from angiogenesis. If we take these effects into account in the model, maybe Hopf bifurcation can be avoided. There are several ways to improving model given in equation (1). One is the dependency of normal cells with the size, which decreases with increasing γ, of the existing vasculature.

For instance, we can deal with intermittent process instead of a continuous process of sprouting from existing blood vessels. We can change the second and fourth equations by

$$\begin{cases} \dfrac{d}{dt}E = \alpha_2 E\left(1 - \dfrac{E}{k_2}\right) - \Phi(t) = \mu_2 E \\ \dfrac{d}{dt}P = \Phi(t) - \delta P - \mu_4 P, \end{cases}$$

where $\Phi(t)$ is the total intermittent sproutings rate. One form of $\Phi(t)$ is

$$\Phi(t) = \sum_{i=0}^{n} \gamma_i \theta(t - \tau_i)\theta(\tau_{i+1} - t)ET,$$

where γ_i and τ_i ($\tau_0 = 0$) are, for $i = 0, \cdots, n$, respectively, the *i-th* sprouting rate and the time interval during which sproutings occur. The Heaviside function $\theta(x)$ is such

that $\theta(x) = 1$ if $x > 0$, and $\theta(x) = 0$, otherwise. To be intermittent, we must have $\gamma_{2i} > 0$ and $\gamma_{2i+1} = 0$, that is, sproutings occur in the time interval $[0, \tau_1]$ with rate γ_0, do not occur in the interval $[\tau_1, \tau_2]$, and so on. Another possibility is

$$\Phi(t) = \sum_{i=0}^{n} s_i \delta(t - \tau_i) E,$$

where s_i and τ_i are, for $i = 0, \cdots, n$, respectively, the *i-th* proportion of epithelial cells generating sproutings and the time at which sproutings occur. The proportion s_i can depend on T. Vaccination campaigns against viral infections were analyzed considering age interval vaccination (Heaviside function) [25] or a series of pulses (Dirac function) [26].

Another improvement of the model (1) is the introduction of the immune response. This can be done by introducing lymphocyte cells action as Nani and Freedman dealt with [11].

In the model (1), chemotherapy that acts specifically against tumor cells can be introduced easily. An intermittent chemotherapy can be introduced in the model by adding one term in the first equation, that is,

$$\frac{d}{dt}T = \alpha_3 AT\left(1 - \frac{T}{k_3}\right) - \beta_2 CT - \mu_3 T - \mu_Q \frac{TQ}{k_q + Q},$$

and adding an equation for the drug administration as

$$\frac{d}{dt}Q = q(t) - l\mu_Q \frac{TQ}{k_q + Q} - \mu_q Q,$$

where Q is the concentration of drug at time t, and μ_Q and μ_q are the rates of, respectively, intake of drug by cancer cells and elimination of drug by body. The parameter l is the amount of drugs intake by one cancer cells, and $q(t)$ is the drug administration rate. The kinetics of drug intake follows Michaelis-Menten [27]. If $q(t) = q$, a fixed value, we have a continuous regimen of administration. Intermittent drug administration can be considered. First, we can define

$$q(t) = \sum_{i=0}^{n} u_i \delta(t - \tau_i),$$

where u_i is, for $i = 0, \cdots, n$, the *i-th* concentration of drug administered at time τ_i. Another is

$$q(t) = \sum_{i=0}^{n} q_i \theta(t - \tau_i)\theta(\tau_{i+1} - t),$$

where q_i and τ_i are, for $i = 0, \cdots, n$, the *i-th* drug administration rate and the time interval during which drug is administrated. To be intermittent, we must have $q_{2i} > 0$ and $q_{2i+1} = 0$.

In this paper we obtained threshold values, but we did not deal with the effects of controlling mechanisms, which are left to a further work. Briefly, for instance, two parameters can be used in order to control cancer growth. The thresholds of the parameters γ and β_2, named γ^{th} and β_2^{th}, can be managed as follows.

Let us suppose that γ and β_2 have values above and below their respective thresholds. To control cancer, parameters of the model (including dynamics of controls) must be managed to increase γ^{th} to surpass γ, and to decrease β_2^{th} to fall below β_2. Another way to control cancer is acting on the probability of sproutings becoming angiogenesis cells, in order to decrease $\delta/(\delta + \mu_4)$, which can be done by decreasing the rate of transformation from pre-angiogenesis to angiogenesis cells δ and/or increasing the mortality rate μ_4 of pre-angiogenesis cells.

Appendix A: Non-trivial equilibrium point

The non-trivial equilibrium value of cancer cells corresponding to model (1), $\bar{T}$, is the positive solution of the equation (5), that is, $f(T) = g(T)$. The fourth degree polynomial $f(T)$ is such that

$$\begin{cases} f(-\infty) = -\infty \\ f(0) = 0 \\ f(+\infty) = -\infty, \end{cases}$$

and has three non-negative roots: 0, $(\alpha_2 - \mu_2)/\gamma = T_E$, and $k_3 = T_A$ is a double root (see equation (7)). Figure 16 shows the qualitative behavior of $f(T)$: $T_A < T_E$ (a), and $T_A > T_E$ (b). Notice that Figure 16(a) corresponds to higher carrying capacity for cancer cells.

The function $g_1(T)$ is such that

$$\begin{cases} g_1(-\infty) = +\infty \\ g_1(0) = g_0 = k_3\left[\dfrac{\mu_3}{\alpha_3} + \dfrac{\beta_2 k_1}{\alpha_3\alpha_1}(\alpha_1 - \mu_1)\right] > 0 \\ g_1(+\infty) = -\infty, \end{cases} \tag{A.1}$$

and has three positive roots: ε/μ_5, $k_3 = T_A$, and $\dfrac{\alpha_1\mu_3}{\beta_1\beta_2 k_1} + \dfrac{\alpha_1 - \mu_1}{\beta_1} = T_g$ (see equations (7) and (8)). The function $g_2(T)$ is such that

$$\begin{cases} g_2(-\infty) = -\infty \\ g_2(0) = 0 \\ g_2(+\infty) = +\infty, \end{cases}$$

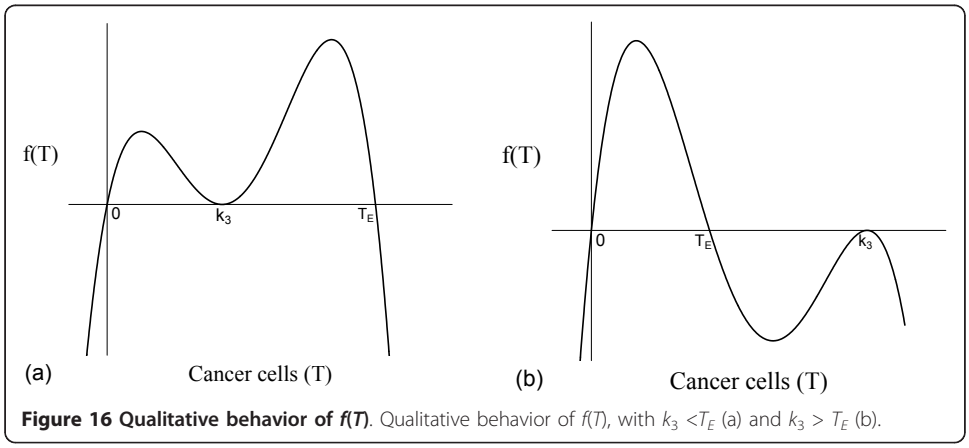

Figure 16 Qualitative behavior of *f(T)*. Qualitative behavior of $f(T)$, with $k_3 < T_E$ (a) and $k_3 > T_E$ (b).

and has two non-negative roots: 0, and $\frac{\alpha_1\mu_3}{\beta_1\beta_2k_1} + \frac{\alpha_1 - \mu_1}{\beta_1} = T_g$ (double root). The dominant terms of the third degree polynomials $g_1(T)$ and $g_2(T)$, when $T \to \pm\infty$, are

$$\begin{cases} g_1(T) = v_1T^3; \text{ with } v_1 = -\dfrac{\varepsilon\beta_1\beta_2k_1}{\mu_5\alpha_3\alpha_1} \\ g_2(T) = v_2T^3; \text{ with } v_2\dfrac{\varepsilon(\beta_1\beta_2k_1)^2k_3}{\mu_5(\alpha_3\alpha_1)^2k_4}. \end{cases}$$

The third degree polynomial $g(T)$ is sum of $g_1(T)$ and $g_2(T)$. Notice that, for $T \geq 0$, we have $g_2(T) \geq 0$, while $g_1(T)$ changes signal. Hence, the effect of $g_2(T)$ in the sum ($g(T)$) is the increasing in the values of $g_1(T)$, except at $T = T_g$, at which we have $g_1(T_g) = g_2(T_g)$. The asymptotic behavior of the polynomial $g(T)$ depends on the velocities of increasing v_2 and v_2 (or coefficients) of T^3. When $\beta_1\,\beta_2 < \alpha_3\,\alpha_1\,k_4/(k_1\,k_3)$ (generically referred to as weak interaction between normal and cancer cells when values of β_1 and β_2 are proportional), in which case T_g is higher, we have

$$\begin{cases} g(-\infty) = +\infty \\ g(0) = g_0 \\ g(+\infty) = -\infty. \end{cases}$$

It can be shown that there is one solution or three positive solutions. When $\beta_1\,\beta_2 > \alpha_3\,\alpha_1\,k_4/(k_1\,k_3)$ (generically referred to as strong interaction between normal and cancer cells when β_1 and β_2 are proportional), in which case T_g is lower, we have

$$\begin{cases} g(-\infty) = -\infty \\ g(0) = g_0 \\ g(+\infty) = +\infty, \end{cases}$$

and there is one negative solution and two positive solutions. In both cases T_g is always a positive root of $g(T)$, and g_0 is given by equation (A.1). The existence of other positive solutions depends on the relative position of the roots of $g_1(T)$ and the coefficients of the polynomials.

Figure 17 shows the qualitative behavior of $g(T)$ for small $\beta_1\,\beta_2$ (weak interaction): when T_g is the greatest root of $g_1(T)$, with three positive solutions (a), and one solution (b); when T_g is between the roots ε/μ_5 and k_3, with three positive solutions (c); and when T_g is the smallest root of $g_1(T)$, with three positive solutions (d). T_1 and T_2, the roots of $g_1(T)$, stand for ε/μ_5 and k_3, depending on the relative positions between them. Figure 17(a) and 17(b) shows clearly the effect of $g_2(T)$ increasing $g_1(T)$ and changing the roots of $g(T)$, named T_1^g and T_2^g : $T_1^g > T_1$ and $T_2^g < T_2$, and both T_1^g and T_2^g disappear when $g_2(T)$ is sufficiently higher.

The positive solution of the equation (5) is the intersection between the curves $f(T)$ and $g(T)$, or roots of $f(T)$-$g(T)$. Notice that:

1. We do not have negative solutions, because $f(T) < 0$ and $g(T) > 0$, for $T < 0$, which implies that $f(T) - g(T) < 0$. At $T = 0$ we have $f(0) - g(0) = -g_0 < 0$.
2. We have $f(\infty) - g(\infty) \to -\infty$, even when $g(\infty) \to +\infty$, because $f(T)$ is fourth degree polynomial, and $g(T)$, third degree.

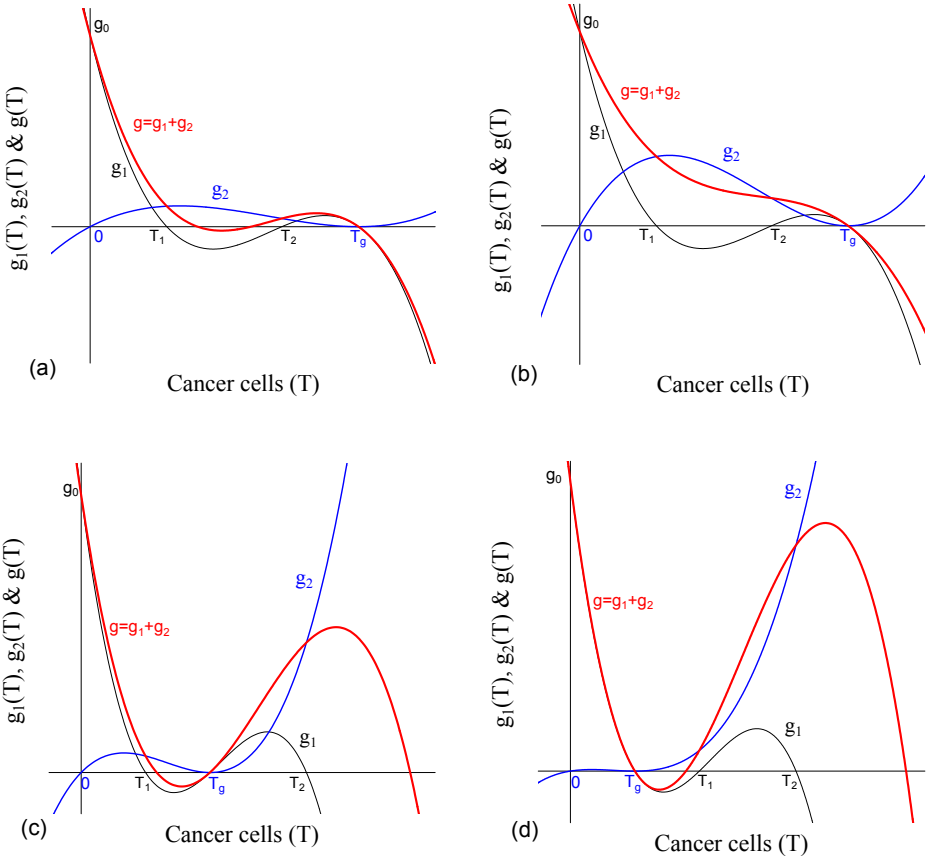

Figure 17 Qualitative behavior of *g*(*T*). Qualitative behavior of $g(T)$, for small β_1 β_2 (weak interaction): T_g is the greatest root of $g_1(T)$, with three positive solutions (a), and one solution (b); T_g is between the roots ε/μ_5 and k_3, with three positive solutions (c); and T_g is the smallest root of $g_1(T)$, with three positive solutions (d). T_1 and T_2, the roots of $g_1(T)$, stand for ε/μ_5 and k_3.

3. $f(T)$ - $g(T)$ is a continuous function, a fourth degree polynomial, where there is not solution for $T < 0$, $f(0)$ - $g(0) < 0$ and $f(\infty)$ - $g(\infty) < 0$. Hence, by the intermediate value theorem, we have 0, 2 or 4 positive solutions in the interval $(0, \infty)$.

4. We are searching biologically feasible equilibrium, hence, according to equation (7), $\bar{T}$ must be lower than the lowest root T_m of $f(T)$, that is, $\bar{T} \in (0, T_m)$, where $T_m = \min\{(\alpha_2 - \mu_2)/\gamma, k_3\}$, the minimum between $(\alpha_2 - \mu_2)/\gamma$ and k_3. Therefore, in the interval $(0, T_m)$ we have at most 2 positive solutions.

Figure 18 shows qualitative behavior of $f(T)$ - $g(T)$. Figures 18(b) and 18(c) (first two lower roots) show two positive solutions satisfying $\bar{T} < T_A, \bar{T} < T_E$ and $\bar{T} < T_g$. Additionally, the constraint $\bar{T} < T_C$ are satisfied, once $\bar{T} < T_g$. Hence, biologically feasible solutions are at most 2. However, Figures 18(c) (last two higher roots) and 18(d) show two positive solutions not biologically feasible, because they are greater than the constraint $T_A = k_3$.

When there is not any positive solution for $f(T)$ - $g(T) = 0$, the unique equilibrium point is the trivial $\bar{Q}^0$. In the case of two positive solutions, the small root $(T_<)$ forms the unstable equilibrium $\bar{Q}^*_<$, and the big one $(T_>)$ forms a possibly stable (let us for

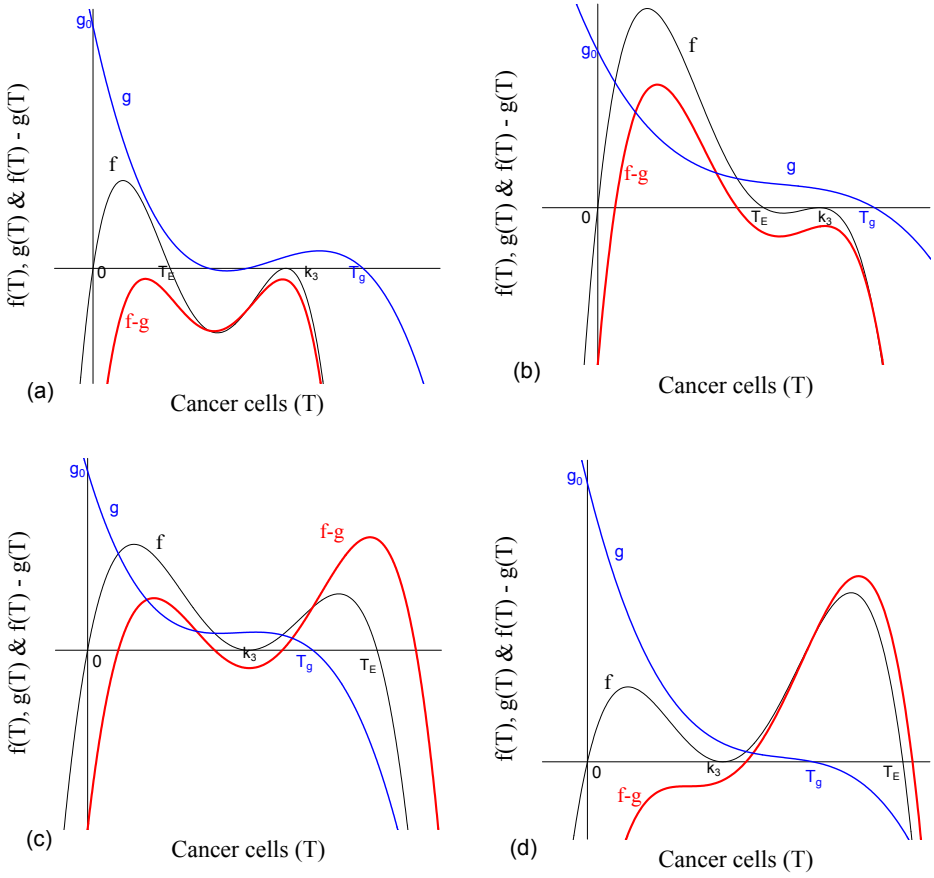

Figure 18 Qualitative behavior of *f*(*T*) - *g*(*T*). Qualitative behavior of *f*(*T*) - *g*(*T*): none (a), two (b) and four (c) solutions. In (d), we show two positive solutions not biologically feasible, because they are greater than the constraint $T_A = k_3$.

simplicity say that it is stable) equilibrium $\bar{Q}^*_>$. Between two stable equilibria $\bar{Q}^*_>$ and $\bar{Q}^0$ (this always exists and is stable), we have an unstable point $\bar{Q}^*_<$. We call as the 'break-point' [28,29] the unstable equilibrium point $\bar{Q}^*_<$, which separates two attracting regions containing one of the equilibrium points $\bar{Q}^*_>$ and $\bar{Q}^0$. In another words, we have a hyper-surface obeying, *e.g.*, $h(\bar{C}(T_<), \bar{E}(T_<), T_<, \bar{P}(T_<), \bar{A}(T_<)) = 0$, generated by the coordinates of the equilibrium point $\bar{Q}^*_<$ such that one of the equilibrium points $\bar{Q}^*_>$ and $\bar{Q}^0$ is an attractor depending on the relative position of the initial conditions supplied to the dynamical system (1) with respect to the hyper-surface h [30].

Appendix B: The local stability of the non-trivial equilibrium $\bar{Q}^c$

Let us show that the matrix A, given by equation (14), is an M-matrix [31] for big non-trivial equilibrium $\bar{Q}^c_>$, where $T_>$is one of the coordinates.

Definition. We say that the $n \times n$ matrix $A = [a_{ij}]$ is a non-singular M-matrix if $a_{ij} \leq 0$, $i \neq j$, and there exists a matrix $B \geq 0$ and a real number $s > 0$ such that

$$A = sI - B \; and \; s > (\rho(B),$$

where I is the identity matrix and ρ is the spectral radius [32].

Or, equivalently:

Proposition 1. A is a non-singular M-matrix if and only if the real part of its eigenvalues is greater than zero.

Proposition 2. A (elements a_{ij}) is a non-singular M-matrix if and only if the diagonal entries are positive, and there exists a positive diagonal matrix D (diagonal elements $d_i > 0$), such that AD is strictly diagonal dominant, that is,

$$a_{ii}d_i > \sum_{j \neq i} |a_{ij}| d_j,$$

for $i = 1, 2, ..., n$.

According to the first part of Proposition 2, the matrix A has positive diagonal elements, see equation (14).

The second part of Proposition 2 is written as

$$\begin{cases} \dfrac{\alpha_2}{k_2}\bar{E}d_1 > \gamma \bar{E} d_2 \\ \dfrac{\alpha_3}{k_3}\bar{A}\bar{T}d_2 > \dfrac{\alpha_3}{k_3}\bar{T}(k_3 - \bar{T})d_1 \\ (\mu_4 + \delta)d_3 > \gamma T d_1 + \gamma \bar{E} d_2 \\ \left(\delta\dfrac{\bar{P}}{\bar{A}} + \dfrac{\varepsilon}{k_4}\bar{A}\bar{T}\right) d_4 > \dfrac{\varepsilon}{k_4}\bar{A}\left|k_4 - \bar{A}\right| d_2 + \delta d_3, \end{cases} \tag{B.1}$$

because $\bar{A}$ can be greater than k_4. The equilibrium values correspond to the point $\bar{Q}^c$, given by equation (9).

Let us define

$$\begin{cases} d_1 = \dfrac{\gamma k_2 + \varphi}{\alpha_2} \\ d_2 = 1 \\ d_3 = \dfrac{\gamma^2 k_2 \bar{T} + \gamma \alpha_2 \bar{E} + (\gamma \bar{T} \alpha_2)\varphi}{\alpha_2(\mu_4 + \delta)} \\ d_4 = \dfrac{\bar{A} - \varphi}{k_3 - \bar{T}}, \end{cases}$$

where $\phi > 0$. By these definitions, the first three inequalities of equation (B.1) hold. To prove the last inequality, we substitute above definitions, and we obtain

$$0 < \varphi < \frac{\varphi_n}{\varphi_d}, \tag{B.2}$$

where the numerator ϕ_n and denominator $\phi_d > 0$ are

$$\begin{cases} \varphi_n = \left(\delta\dfrac{\bar{P}}{\bar{A}} + \dfrac{\varepsilon}{k_4}\bar{A}\bar{T}\right)\dfrac{\bar{A}}{k_3 - \bar{T}} - \dfrac{\varepsilon}{k_4}\bar{A}\left|k_4 - \bar{A}\right| \\ \qquad - \dfrac{\delta\gamma k_2(\alpha_2 - \mu_2)}{\alpha_2(\mu_4 + \delta)} \\ \varphi_d = \left(\delta\dfrac{\bar{P}}{\bar{A}} + \dfrac{\varepsilon}{k_4}\bar{A}\bar{T}\right)\dfrac{1}{k_3 - \bar{T}} + \dfrac{\delta(\gamma\bar{T} + \alpha_2)}{\alpha_2(\mu_4 + \delta)}, \end{cases}$$

with the last term of the numerator being obtained using the relation

$$\gamma^2 k_2 \bar{T} + \gamma \alpha_2 \bar{E} = \gamma k_2(\alpha_2 - \mu_2),$$

which is valid in the equilibrium. Since $\phi_d > 0$, if we show that $\phi_n > 0$, then there exists a positive number ϕ.

Let us consider the case where there are two positive solutions for the equation $f(T) = g(T)$. In this case, we show that the bigger equilibrium $\bar{Q}^c_>$, with coordinate $T_>$as solution of (5), is stable. Additionally, we assume that $\bar{A} > k_4$, which seems reasonable since the equilibrium $\bar{Q}^c$ is stable for $\bar{T} > (\alpha_1 - \mu_1)/\beta_1 = T_C$. Substituting the coordinates of the equilibrium $\bar{Q}^c$, the numerator of ϕ can be written as

$$\varphi_n = \frac{\bar{A}}{(k_3 - \bar{T})^2}\Phi(\bar{T}),$$

with

$$\begin{aligned}\Phi(\bar{T}) = {} & \frac{\varepsilon}{k_4\alpha_3}\Phi_1(\bar{T}) - \frac{\gamma\delta k_2\alpha_3}{\alpha_2(\mu_4+\delta)\mu_3 k_3} \\ & \times (k_3 - \bar{T})^2\Phi_2(\bar{T}),\end{aligned} \tag{B.3}$$

where

$$\begin{cases}\Phi_1(\bar{T}) = k_4\alpha_3\bar{T}^2 - 2k_3(k_4\alpha_3 - \mu_3)\bar{T} \\ \qquad\qquad +k_3^2(k_4\alpha_3 - \mu_3) \\ \Phi_2(\bar{T}) = \gamma\bar{T}^2 - 2(\alpha_2 - \mu_2)\bar{T} + (\alpha_2 - \mu_2),\end{cases}$$

and we must show that $\Phi(\bar{T}) > 0$, for higher value of $\bar{T}$, that is, $\bar{T} = T_>$. Let us assume that $k_4\alpha_3 > \mu_3$. Then, we have $\Phi(\bar{T}) > 0$, for $\bar{T} \geq 0$, because the discriminant of $\Phi_1(\bar{T})$ is

$$\Delta_1 = -4k_3^2\mu_3(k_4\alpha_3 - \mu_3) < 0.$$

Hence, $\Phi_2(\bar{T})$ determines the existence of positive ϕ_n. The discriminant of $\Phi_2(\bar{T})$ is

$$\Delta_2 = 4_\gamma(\alpha_2 - \mu_2)(T_E - T_A),$$

where T_E and T_A are given in equation (7). We have two possibilities. First, when $T_E < T_A$, we have $\Phi_2(\bar{T}) > 0$, for all $\bar{T} \geq 0$, and $\Phi(\bar{T}) > 0$ for

$$\varepsilon > \varepsilon_{\min},$$

where

$$\varepsilon_{\min} = \frac{\gamma\delta k_2\alpha_3 k_4\alpha_3}{\alpha_2(\mu_4+\delta)\mu_3 k_3}(k_3 - T_>)^2\frac{\Phi_2(T_>)}{\Phi_1(T_>)}. \tag{B.4}$$

Hence, when $\varepsilon > \varepsilon_{\min}$, $\phi_n > 0$ and we have a positive number ϕ obeying equation (B.2). Second, when $T_E > T_A$, $\Phi_2(\bar{T})$ has two positive solutions $\Phi_{2<}$and $\Phi_{2>}$given by

$$\begin{cases} \Phi_{2<} = \dfrac{\alpha_2-\mu_2}{\gamma} - \sqrt{\dfrac{\alpha_2-\mu_2}{\gamma}\left(\dfrac{\alpha_2-\mu_2}{\gamma}-k_3\right)} \\ \quad = T_E - \sqrt{T_E(T_E-T_A)} \\ \Phi_{2>} = \dfrac{\alpha_2-\mu_2}{\gamma} + \sqrt{\dfrac{\alpha_2-\mu_2}{\gamma}\left(\dfrac{\alpha_2-\mu_2}{\gamma}-k_3\right)} \\ \quad = T_E + \sqrt{T_E(T_E-T_A)}, \end{cases}$$

and we have $\Phi_2(\bar{T}) \le 0$, for $\Phi_{2<} \le \bar{T} \ge \Phi_{2>}$; otherwise, $\Phi_2(\bar{T}) > 0$. Notice that $\Phi_{2>}$is out of the range of feasibility, once $\Phi_{2>} > T_E$. We know that $(\alpha_1-\mu_1)/\beta_1 < \bar{T} < k_3$, but the bigger solution under consideration is $T_> = (\alpha_1-\mu_1)/\beta_1^c = T_E^c$, for $\beta_1 \ge \beta_1^c$. It is easy to show that $\Phi_2(k_3) < 0$; but, $\Phi_2(T_E^c) \le 0$, if $T_E^c \ge \Phi_{2<}$, and $\Phi_2(T_E^c) > 0$, if $T_E^c < \Phi_{2<}$. Hence, $\Phi_2(\bar{T}) \le 0$ if $T_E^c < \Phi_{2<}$. Hence, $\Phi(\bar{T}) > 0$, for $\bar{T} \ge 0$, when $T_E^c \ge \Phi_{2<}$, or when $T_E^c \ge \Phi_{2<}$ and $\bar{T} \ge \Phi_{2<}$; and $\Phi(\bar{T}) > 0$, when $T_E^c < \Phi_{2<}$ and $T_E^c < \bar{T} < \Phi_{2<}$ for $\varepsilon > \varepsilon_{\min}$.

Summarizing, $\phi_n > 0$ occurs, in order to have positive number ϕ:

1. $T_A < T_E$ or $\gamma < (\alpha_2 - \mu_2)/k_3$ - weak capacity of recruitment of the normal epithelial cells by cancer cells. We have:

1.a *If* $T_E^c \ge \Phi_{2<}$: $\varphi_n > 0$ without restriction about $T_>$.

1.b If $T_E^c < \bar{T} < \Phi_{2<}$: we have two possibilities

1.b.1 If $T_> > \Phi_{2<}$: $\phi_n > 0$ without restriction about $T_>$.

1.b.2 If $T_> < \Phi_{2<}$: $\phi_n > 0$ if $\varepsilon > \varepsilon_{\min}$, where $T_>$satisfies $\varepsilon_{\min}$, equation (B.4). Higher proliferation of angiogenesis cells must occur.

2. $T_A > T_E$ or $\gamma > (\alpha_2 - \mu_2)/k_3$ - strong capacity of coopting normal epithelial cells by cancer cells: $\phi_n > 0$, if $\varepsilon > \varepsilon_{\min}$, where $T_>$satisfies $\varepsilon_{\min}$.

When γ is small, the big equilibrium $\bar{Q}_>^c$, with one coordinate $T_>$, is stable without conditions (cases 1.a and 1.b.1). However, for sufficiently higher values of γ, the big equilibrium point $\bar{Q}_>^c$ can be unstable (case 2), in which case Hopf bifurcation can occur (see Appendix C).

In the case of the small equilibrium $\bar{Q}_<^c$, with one coordinate $T_<$, it is unstable. Assuming that $\bar{A} < k_4$, we show here that A corresponding to small $T_<$is not an M-matrix (we are not proving that $\bar{Q}_<^c$ is unstable). In this case, equation (B.3) becomes

$$\Phi(\bar{T}) = -\frac{\varepsilon}{k_4\alpha_3}\Phi_1(\bar{T}) - \frac{\gamma\delta k_2\alpha_3}{\alpha_2(\mu_4+\delta)\mu_3 k_3} \times (k_3-\bar{T})^2\Phi_2(\bar{T}),$$

where

$$\begin{cases} \Phi_1(\bar{T}) = k_4\alpha_3(\bar{T}-k_3)^2 - \mu_3 k_3^2 \\ \Phi_2(\bar{T}) = \gamma\bar{T}^2 - 2(\alpha_2-\mu_2)\bar{T} + (\alpha_2-\mu_2). \end{cases}$$

The bigger roots of $\Phi_1(\bar{T})$ and $\Phi_2(\bar{T})$ are not biologically feasible, because they are, respectively, higher than k_3 and $(\alpha_2 - \mu_2)/\gamma$. Let us define $T_m = \min\{T^1_<, T^2_<\}$, where $\min\{T^1_<, T^2_<\}$ is the minimum between the small roots of, respectively, $\Phi_1(\bar{T})$ and $\Phi_2(\bar{T})$ given by $T^1_< = k_3\left(1 - \sqrt{1 - \frac{\mu_3}{k_4\alpha_3}}\right)$, assuming that $k_4 \geq 1$, and $T^2_< = T_E\left(1 - \sqrt{1 - \frac{T_A}{T_E}}\right)$, assuming that $T_E \geq T_A$. Hence, if $\bar{T} < T_m$, we have $\Phi(\bar{T}) > 0$ and there is not a positive number ϕ. Notice that, when $T_E < T_A$, we have $\Phi_2(\bar{T}) > 0$, and it is enough to satisfy $\bar{T} < T^1_<$.

Appendix C: Hopf bifurcation

In Figures 19, 20 and 21 we illustrate the Hopf bifurcation (see Figure 10 in the main text), using values of parameters given in Table 2, except γ assuming higher values. The following figures are mathematical results, not cancer in an organ.

Dynamical trajectories are shown in Figure 19 for γ near γ_1^c : $\gamma_1 = 2.31 \times 10^{-2} \lesssim \gamma_c^1$ and $\gamma_2 = 2.32 \times 10^{-2} \gtrsim 10^{-2} \gtrsim \gamma_1^c$. When $T(0) = 0.44$, trajectories of both cases go to $\bar{Q}^0$ (trajectories similar to Figure 1(a), not shown). When $T(0) = 0.45$, dynamical trajectories for γ_1 go to stable $\bar{Q}^*_>$ (a), while for γ_2, they oscillate around unstable $\bar{Q}^*_>$ (b), in which case limit cycle arises.

Now, we show the dynamical trajectories for γ near γ_2^c. Again, for $\gamma_3 = 2.519 \times 10^{-2} \lesssim \gamma_2^c$ and $\gamma_4 = 2.520 \times 10^{-2} \gtrsim \gamma_2^c$, when $T(0) = 0.41$, trajectories of both cases go to $\bar{Q}^0$ (trajectories similar to Figure 1(a), not shown). When $T(0) = 0.42$, Figure 20 shows dynamical trajectories for γ_3 oscillating around unstable $\bar{Q}^*_>$. Notice that the amplitude of regular oscillations of the variables is very high: C and E (a), T (b), P (c) and A (d). For the same $T(0) = 0.42$, we show the dynamical trajectories for γ_4 and $\gamma_5 = 2.519675 \times 10^{-2}$, which is slightly higher than γ_2^c. In both cases we have

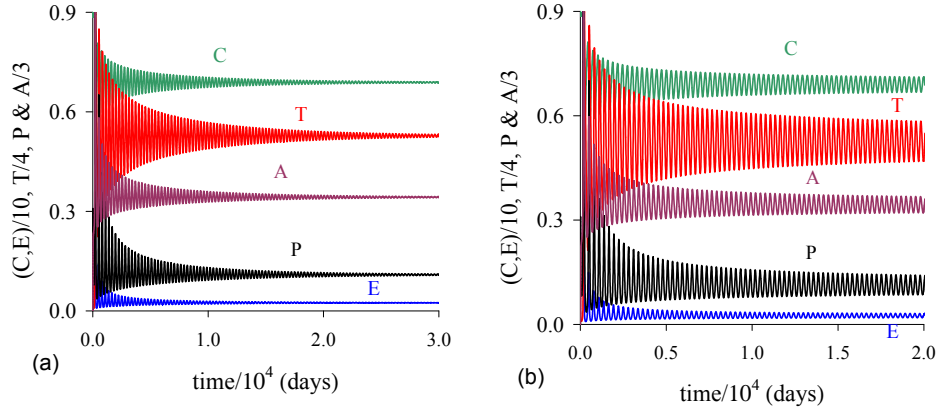

Figure 19 Dynamical trajectories using γ near γ_1^c. Dynamical trajectories of the system (1) considering the values of parameters given in Table 2, except γ near γ_1^c. When $T(0) = 0.45$ (for $T(0) = 0.44$ both cases go to $\bar{Q}^0$), $\bar{Q}^*_>$ is the attracting point for $\gamma = 2.31 \times 10^{-2}$ (a), and limit cycle with small amplitude circulating unstable $\bar{Q}^*_>$ appears for $\gamma = 2.32 \times 10^{-2}$ (b). The scales of vertical and horizontal axes must be multiplied by the factors shown in the legends to obtain the actual values.

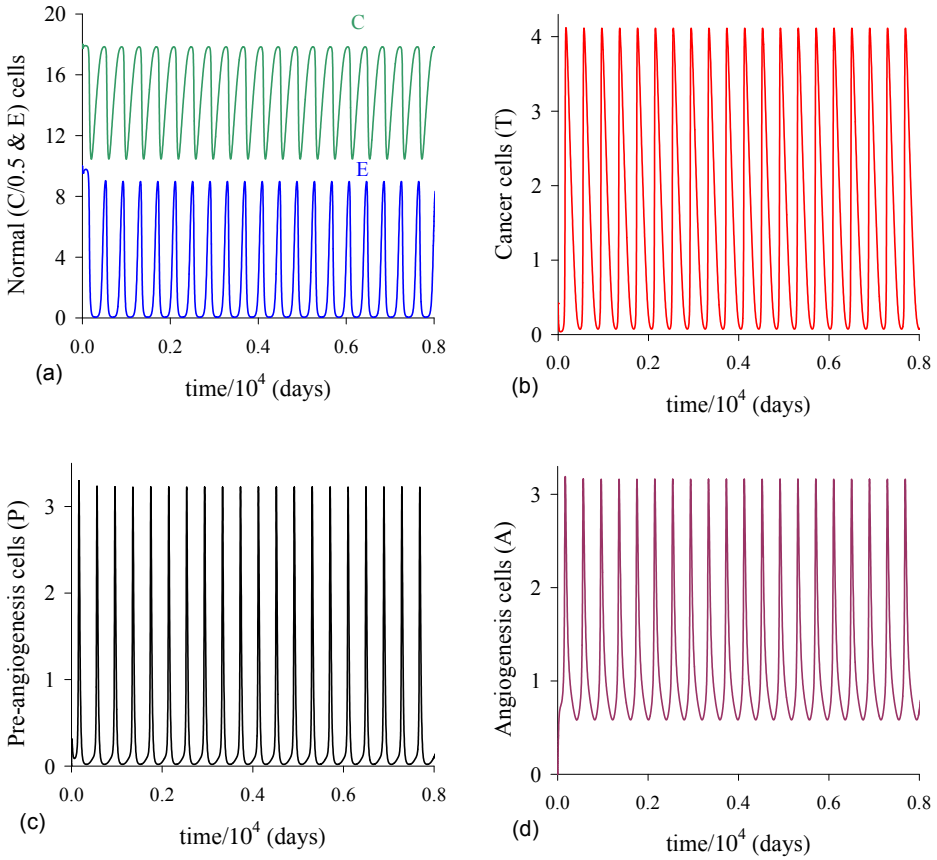

Figure 20 Dynamical trajectories using γ near but lower than γ_2^c. Dynamical trajectories of the system (1) considering the values of parameters given in Table 2, except γ near but lower than γ_2^c. When $T(0) = 0.42$ ($\bar{Q}^0$ is attracting for $T(0) = 0.41$), limit cycle with large amplitude circulating unstable $\bar{Q}^*_>$ occurs for $\gamma = 2.519 \times 10^{-2}$. Regular oscillations are observed in all variables: C and E (a), T (b), P (c) and A (d). The scales of vertical and horizontal axes must be multiplied by the factors shown in the legends to obtain the actual values.

$\bar{Q}^*_>$, and Figure 21 shows trajectories going to $\bar{Q}^0$ with different number of oscillations: for γ_4 (a), we have one oscillation, while for γ_5, three oscillations, showing C and E (b), T (c), P and A (d). When $\gamma > \gamma_2^c$, we observe that E goes initially to zero, and, after 400 *days*, increases abruptly, according to Figure 21(a). In Figure 5(a) we showed that C has similar behavior.

Comparing Figures 19, 20 and 21, we observe that, as γ increases, the real part of the complex eigenvalues decreases (see Table 3), and damped oscillations persist for longer times. At $\gamma = \gamma_1^c$, real part is zero. For instance, a pair of complex number has real part -2.3×10^{-7} at $\gamma = 2.3196 \times 10^{-2}$, and $+9.0 \times 10^{-7}$ at $\gamma = 2.3197 \times 10^{-2}$. In both cases, two of them are complex number with negative real part and one negative number. As γ increases sinceafter γ_1^c, amplitude of the limit cycle increases, and at $\gamma = \gamma_2^c$ disappears. Observe that a finite number of oscillations occurs before reaching the trivial equilibrium. The increasing in the amplitude of regular oscillations resulted in an unsustainable value of $T_>$, and, hence, this value (due to being lower than a critical value) can not trigger new burst of cancer cells.

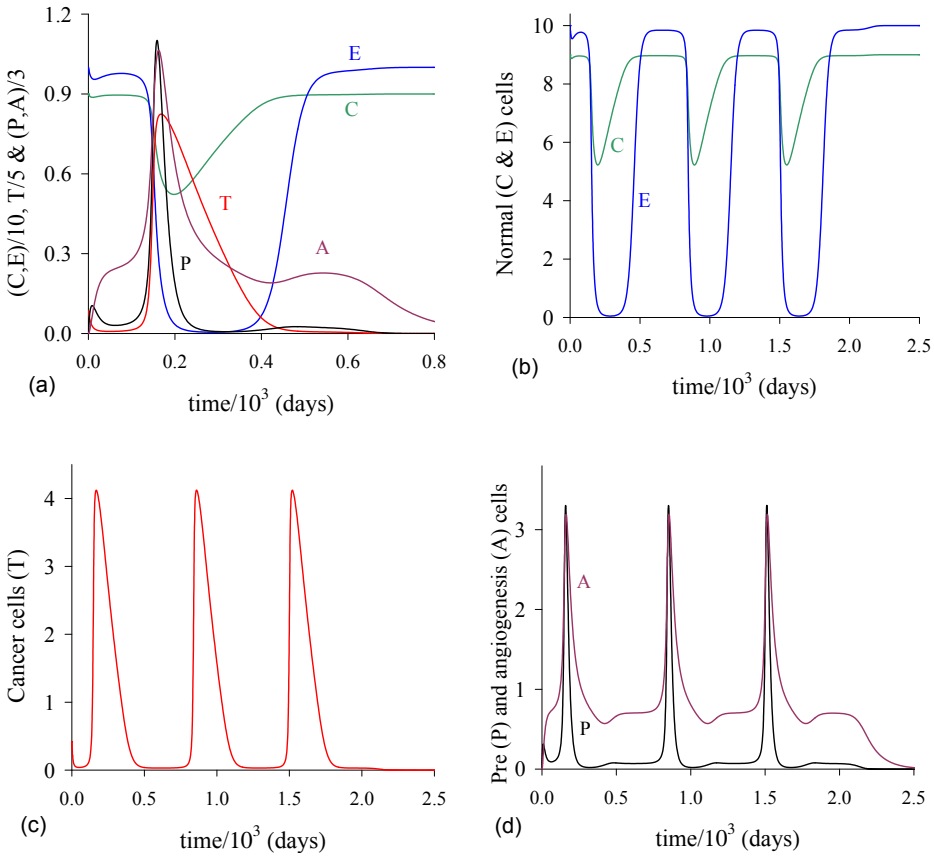

Figure 21 Dynamical trajectories using γ near but greater than γ_2^c. Dynamical trajectories of the system (1) considering the values of parameters given in Table 2, except γ near but greater than γ_2^c. When $T(0) = 0.42$ ($\bar{Q}^0$ is attracting for $T(0) = 0.41$), limit cycle disappears for $\gamma = 2.520 \times 10^{-2}$. Being $\bar{Q}^*_>$ unstable, the dynamical trajectories go to trivial $\bar{Q}^0$ after one oscillation (a). However, the number of oscillations increases if γ is very close to γ_2^c. For $\gamma = 2.519675 \times 10^{-2}$ and $T(0) = 0.42$, $\bar{Q}^0$ is attained after three oscillations: *C* and *E* (b), *T* (c), *P* and *A* (d). The scales of vertical and horizontal axes must be multiplied by the factors shown in the legends to obtain the actual values.

Numerical results regarding to γ showed that there is a threshold for γ, plus two critical values. For small values, $\gamma < \gamma^{th}$, cancer cells can not induce new blood vessels, and cancer fades out. As γ increases, amplitude of damped oscillations increases and appears stable limit cycle. The limit cycle separates cancer state ($\bar{Q}^*$) to cure ($\bar{Q}^0$). However, the cure occurs at the expense of death of cancer cells due to elimination of the pre-existing network of blood vessels. This phenomenon occurs due to the absence of dependency between normal cells (*C*) and pre-existing epithelial cells (*E*) in the carrying capacities k_1 and k_2.

Acknowledgements
This work was supported by a grant from FAPESP (Projeto Temático). HMY gratefully acknowledges a Fellowship awarded by CNPq. HMY thanks PFA Mancera for careful reading of the manuscript and providing corrections.

Competing interests
The authors declare that they have no competing interests.

Received: 28 September 2011 Accepted: 2 February 2012 Published: 2 February 2012

References

1. Jemal A, Siegel R, XJ Q, Ward E: **Cancer Statistics, 2010.** *CA Cancer J Clin* 2010, **60**:277-300.
2. Parkin DM, Pisani PJF: **Global Cancer Statistics.** *CA Cancer J Clin* 1999, **49**:33-64.
3. Sompayrac L: *How Cancer Works* Boston: Jones and Bartlett Publishers; 2004.
4. Byrne HM: **Using mathematics to study solid tumour growth.** *Proceedings of the 9th General Meetings of European Women in Mathematics* 1999, 81-107.
5. Araujo RP, McElwain DLS: **A History of the Study of Solid Tumour Growth: The Contribution of Mathematical Modelling.** *Bull Math Biol* 2004, **66**:1039-1091.
6. Michelson S, Leith JT: **Positive Feedback and Angiogenesis in Tumor Growth Control.** *Bull Math Biol* 1997, **59**:233-254.
7. d'Onofrio A, Gandolfi A: **Tumour Eradication by Antiangiogenic Therapy: Analysis and Extensions of the Model by Hahnfeldt et al. (1999).** *Math Biosc* 2004, **191**:159-184.
8. Risau W: **Mechanisms of Angiogenesis.** *Nature* 1997, **386**:671-674.
9. Chaplain MAJ, McDougall SR, Anderson ARA: **Mathematical Modeling of Tumor-Induced Angiogenesis.** *Annu Rev Biomed Eng* 2006, **8**:233-257.
10. Edelstein-Keshet L: *Mathematical Models in Biology* New York: McGraw Hill, Inc; 1988.
11. Nani F, Freedman HI: **A mathematical Model of Cancer Treatment by Immunotherapy.** *Math Biosc* 2000, **163**:159-199.
12. Ruggiero RA, Bustoabad OD: **The Biological Sense of Cancer: A Hypothesis.** *Theoret Biol Med Modelling* 2006, **3**:43:1-14.
13. Kitagawa M, Utsuyama M, Kurata M, Yamamoto K, Yuasa Y, Ishikawa Y, Arai T, Hirokawa K: **Cancer and Aging: Symposium of the 27th Annual Meeting of the Japanese Society for Biomedical Gerontology.** *Tokyo Cancer Immunol Immunother* 2005, **54**:623-634.
14. Komarova NL, Mironov V: **On The Role of Endothelial Progenitor Cells in Tumor Neovascularization.** *J Theoret Biol* 2005, **235**:338-349.
15. Murray JD: *Mathematical Biology* New York: Springer-Verlag; 1989.
16. Press WH, Flannery BP, Teukolsky SA, Vetterling WT: *Numerical Recipes The Arts of Scientifc Computing (FORTRAN Version)* Cambridge: Canbridge University Press; 1989.
17. Kuznetsov YA: *Elements of Applied Bifurcation Theory* New York: Springer-Verlag; 1995.
18. Agur Z, Larakelyan L, Daugulis P, Ginosar Y: **Hopf Point Analysis for Angiogenesis Model.** *Discr Contin Dynam Syst* 2004, **4(1)**:29-38.
19. Peirce SM: **Computational and Mathematical Modeling of Angiogenesis.** *Microcirculation* 2008, **15(8)**:739-751.
20. Chaplain MAJ: **Mathematical Modelling of Angiogenesis.** *J Neuro-Oncology* 2000, **50**:37-51.
21. Ribba B, Colin T, Schnell S: **A Multiscale Mathematical Model of Cancer, And Its Use in Analyzing Irradiation Therapies.** *Theoret Biol Med Modelling* 2006, **3**:7:1-19.
22. Budu-Grajdeanu P, Schugart RC, Friedman A, Valentine C, Agarwal AK, Rovin BH: **A Mathematical Model of Venous Neointimal Hyperplasia Formation.** *Theoret Biol Med Modelling* 2008, **5**:2:1-9.
23. Arakelyan L, Vainstein V, Agur Z: **A Computer Algorithm Describing The Process of Vessel Formation and MAturation, and Its Use for Predicting The Effects of Anti-angiogenic and Anti-maturation Therapy on Vascular Tumor Growth.** *Angiogenesis* 2002, **5**:203-214.
24. Stamatakos GS, Kolokotroni EA, Dionysiou DD, Geordiadi EC, Desmedt C: **An Advanced Discrete State-Discrete Event Multiscale Simulation Model of The Response of A Solid Tumor to Chemotherapy: Mimicking a Clinical Study.** *J Theoret Biol* 2010, **266**:124-139.
25. Yang HM: **Modeling Directly Transmitted Infections in a Routinely Vaccinated Population - The Force of Infection Described by Volterra Integral Equation.** *Appl Math Comput* 2001, **122(1)**:27-58.
26. Yang HM: **Modelling Vaccination Strategy Against Directly Transmitted Diseases Using a Series of Pulses.** *J Biol Syst* 1998, **6(2)**:187-212.
27. Kenner J, Sneyd J: *Mathematical Physiology* New York: Springer; 1998.
28. Bradley DJ, May RM: **Consequences of Helminth Aggregation for the Dynamics of Schistosomiasis.** *Trans R Soc Trop Med Hyg* 1978, **73**:262-273.
29. May RM: **Togetherness Amongst Schistosome: Its Effects on the Dynamics of the Infection.** *Math Biosc* 1977, **35**:301-343.
30. Esteva L, Yang HM: **Mathematical Model to Assess the Control of *Aedes aegypti* Mosquitoes by The Sterile Insect Technique.** *Math Biosc* 2005, **198**:132-147.
31. Raimundo SM, Massad E, Yang HM: **Modelling Congenital Transmission of Chagas' Disease.** *BioSystems* 2010, **99**:215-222.
32. Berman A, Plemmons RJ: *Nonnegtive Matrices in the Mathematical Sciences* New York: Academic Press; 1979.

doi:10.1186/1742-4682-9-2
Cite this article as: Yang: **Mathematical modeling of solid cancer growth with angiogenesis.** *Theoretical Biology and Medical Modelling* 2012 **9**:2.